JGR Oceans

RESEARCH ARTICLE
10.1029/2022JC018689

Vertically Resolved Pelagic Particle Biomass and Size Structure Across a Continental Shelf Under the Influence of a Western Boundary Current

Hayden T. Schilling[1,2,3], Jason D. Everett[2,4], Amandine Schaeffer[2,5], Charles Hinchliffe[1,2], Peter Yates[1,2], Mark E. Baird[6], and Iain M. Suthers[1,2]

[1]Sydney Institute of Marine Science, Mosman, NSW, Australia, [2]Centre for Marine Science & Innovation, Kensington, NSW, Australia, [3]Now at New South Wales Department of Primary Industries, Port Stephens Fisheries Institute, Taylors Beach, NSW, Australia, [4]School of Mathematics and Physics, University of Queensland, Brisbane, QLD, Australia, [5]School of Mathematics and Statistics, Kensington, NSW, Australia, [6]Commonwealth Scientific and Industrial Research Organisation, Battery Point, TAS, Australia

Abstract Continental shelves are key to societal interactions with the oceans, supporting >90% of the world's fisheries through highly productive ecosystems. Previous research has shown that phytoplankton biomass is generally higher on the inner continental shelves, often due to increased nutrient inputs from upwelling or coastal run-off. However, consistency in observed vertical and horizontal gradients (in abundance, biomass or size) of larger particulates, including zooplankton, on continental shelves has not been established. Using an optical plankton counter and CTD mounted on an undulating towed body, we present high-resolution vertically resolved profiles of pelagic particle size structure across a continental shelf. Biomass was highest inshore, declining with distance from shore and with depth in the top 100 m of the water column, although the presence of frontal zones can alter this pattern. In the region adjacent to the East Australian Current (EAC), uplift generated by either the EAC interacting with the continental slope or upwelling-favorable winds, correlated with smaller geometric mean sizes and steeper size spectrum slopes, particularly in the presence of frontal features. South of the EAC separation, the continental shelf water mass was more homogenous but still displayed the same horizontal and vertical patterns in particulate biomass and mean size. By combining our observations in a global comparison, we demonstrate consistent particulate distributions on continental shelves where the inner shelf has higher biomass with a steeper size spectrum slope compared to offshore. The highly productive inner shelf supports zooplankton communities vital to temperate ecosystems and coastal fisheries, through their consistently high biomass.

Plain Language Summary It is commonly accepted that chlorophyll *a* and phytoplankton are more abundant on continental shelves compared to the open ocean due to nutrient enrichment from either upwelling or terrestrial inputs. Little is known about the consistency in larger particulates, including zooplankton. We present the first depth resolved cross-shelf transects of zooplankton sized particulates. We show globally consistent patterns where close to the coast there is higher abundance and biomass, smaller geometric mean size and a steeper size spectrum slope representing a more productive community.

Key Points:

- We present the first depth resolved cross-shelf transects of the abundance, biomass, and geometric mean size of particulate matter
- Higher biomass and abundance were generally found close to the coast likely representing a more productive community
- These patterns were consistent globally but can show significant small-scale variation around frontal zones

Supporting Information:

Supporting Information may be found in the online version of this article.

Correspondence to:

H. T. Schilling,
hayden.schilling@dpi.nsw.gov.au

Citation:

Schilling, H. T., Everett, J. D., Schaeffer, A., Hinchliffe, C., Yates, P., Baird, M. E., & Suthers, I. M. (2023). Vertically resolved pelagic particle biomass and size structure across a continental shelf under the influence of a western boundary current. *Journal of Geophysical Research: Oceans*, *128*, e2022JC018689. https://doi.org/10.1029/2022JC018689

Received 28 MAR 2022
Accepted 22 JAN 2023

Author Contributions:

Conceptualization: Jason D. Everett, Amandine Schaeffer, Mark E. Baird, Iain M. Suthers
Formal analysis: Hayden T. Schilling
Investigation: Hayden T. Schilling, Mark E. Baird, Iain M. Suthers
Methodology: Amandine Schaeffer
Visualization: Hayden T. Schilling, Amandine Schaeffer
Writing – original draft: Hayden T. Schilling

1. Introduction

Continental shelves account for less than 7% of the earth's ocean surface area yet support over 90% of the world's fisheries catch (Pauly et al., 2002). These fisheries are based upon high primary productivity (Bakun & Weeks, 2008; Mackinson et al., 2009; Marshak & Link, 2021) which is transferred into fisheries species via zooplankton (Mitra et al., 2014). While primary productivity and chlorophyll *a* on continental shelves have been quantified via highly accessible satellite imagery (Everett et al., 2014; Marshak & Link, 2021), zooplankton dynamics on continental shelves, which are a more direct link to higher trophic levels remains uncertain. Understanding of cross-shelf dynamics of zooplankton is largely limited to the Atlantic Ocean (Marcolin et al., 2013; Sourisseau & Carlotti, 2006; Vandromme et al., 2014), with limited understanding of general patterns of variability across continental shelves. As fisheries face increasing pressure, it is important to understand the drivers of fisheries productivity including zooplankton, which has been shown to support over 50% of coastal fish biomass (Holland et al., 2020; Maia et al., 2018; Truong et al., 2017).

Writing – review & editing: Jason D. Everett, Amandine Schaeffer, Charles Hinchliffe, Peter Yates, Mark E. Baird, Iain M. Suthers

The transfer of energy between trophic levels through predation is largely driven by size (Barnes et al., 2010), and the size frequency distribution or size spectrum of a community can provide valuable insight into these trophic dynamics (Blanchard et al., 2017). The size of all individuals in a community, irrespective of species identity, can be described by the size spectrum that is typically strongly right-skewed with many small individuals, and fewer large individuals (Blanchard et al., 2017; Heneghan et al., 2019). On log-log axes, the negative linear slope of the zooplankton size spectrum (Edwards et al., 2017; Sprules & Barth, 2015), provides insight into energy transfer and community function (Atkinson et al., 2021; White et al., 2007). The size spectrum implicitly reflects the outcome of ecological processes including predation, the growth of individuals through different size classes, and the repopulation of smaller size classes through reproduction (Andersen et al., 2016; Blanchard et al., 2017; Sprules & Barth, 2015). While there is variability in interpretations of size spectrum depending on the size of particles in the spectrum due to sampling efficiency and natural "dome shapes'" in some communities (Marcolin et al., 2013; Rossberg et al., 2019), within the mesozooplankton size range (≈0.2–3 mm Equivalent Spherical Diameter; ESD), the elevation of the spectrum reflects the environmental effects which influence the overall production and biomass of a community (Irigoien et al., 2009; Zhou, 2006). By quantifying the gradients in particulate size structure, such as with an Optical Plankton Counter (OPC, Herman, 1992) which counts and measures particles in the size range dominated by mesozooplankton, it is possible to investigate spatial variation in productivity, trophic dynamics and community structure.

Spatial patterns in mesozooplankton (henceforth zooplankton) size spectrum slopes have been examined across several continental shelves, and generally correlate with patterns of increased primary productivity in the inner shelf (Lucas et al., 2011). In the southwest Atlantic, the zooplankton community on the continental shelf was characterized by higher biomass and a steeper zooplankton size spectrum slope compared to offshore oceanic stations (Marcolin et al., 2013). Stratification of the water column offshore was also associated with higher biomass at depth (Marcolin et al., 2013). This is similar to the northeast Atlantic where high zooplankton biomasses and steeper zooplankton size spectrum slopes were found in some but not all inshore regions, most often in the lower salinity, higher chlorophyll *a* coastal water, indicating potential effects of freshwater discharge (Irigoien et al., 2009; Sourisseau & Carlotti, 2006; Vandromme et al., 2014). Fewer studies have examined the vertical patterns of zooplankton on continental shelves and this remains a key knowledge gap despite widespread recognition of variation in vertical distributions of zooplankton often attributed to diel vertical migration (Lampert, 1989), and the three-dimensional influences of continental shelf oceanography (Schaeffer et al., 2013).

Along continental shelves there are multiple drivers of productivity including boundary currents. Eastern boundary currents directly supply nutrient rich, cool waters from the poles toward the equator which then interact with wind driven upwelling to produce some of the most productive fisheries in the world, including those located in the Humboldt and California currents (Carr & Kearns, 2003). By contrast, western boundary currents (WBCs) are narrow currents which swiftly move warm oligotrophic water poleward. When WBCs interact with the adjacent continental shelf they induce upwelling of cold nutrient rich water on the inshore edge through bottom stress, and generate strong frontal regions (Aguiar et al., 2014; Everett et al., 2012; Schaeffer et al., 2013, 2014). These processes often facilitate a nutrient and productivity gradient from oligotrophic WBCs across the continental shelves into the coast (Everett et al., 2014; Kobari et al., 2018; Schaeffer et al., 2013). The interaction of the WBC and continental shelf water creates new vertical or horizontal pathways by which nutrients and biological materials enter and leave the continental shelf system (Malan et al., 2020).

The WBC of the South Pacific Ocean is the East Australian Current (EAC). It generates eddies (Everett et al., 2012; Schaeffer et al., 2017), and drives upwelling and isotherm uplift as it interacts with the continental shelf (Roughan & Middleton, 2002). These oceanographic processes influence nutrient availability and the biomass of chlorophyll *a*, generating spatially persistent features. A spring bloom is observed south of 34°S as the EAC weakens and the nutrient rich Tasman Sea water intrudes, with more stable lower chlorophyll *a* levels observed to the north (Everett et al., 2014). To date, there are no studies quantifying the general cross-shelf or vertical distribution of pelagic particles in the EAC region. Here we investigate horizontal and vertical patterns in particulate size structure using four high-resolution vertically resolved, cross-shelf transects of particulates on the eastern continental shelf of Australia to:

1. Identify latitudinal differences in particulate size structure across the continental shelf in relation to the EAC, and
2. Examine the potential drivers of the observed patterns in particulate biomass and size structure, and

3. Relate our observations to previous research to propose a general concept of mesozooplankton-sized particulate size structure on continental shelves globally.

2. Materials and Methods

2.1. Voyage Context and Seasonal Variation in Oceanography

The EAC is the WBC of the South Pacific gyre, forming between 10°S and 20°S where the South Equatorial Current bifurcates off the Great Barrier Reef and north-eastern Australia (Ridgway & Dunn, 2003). The southward flowing component forms the EAC, a consistent southward jet, flowing at 0.8–1.5 m s^{-1} along the continental shelf with a maximum core velocity and a slight widening in summer (Archer et al., 2017). The majority of the EAC separates from the coast between approximately 30°–32°S and flows eastward as the EAC eastern extension (Cetina-Heredia et al., 2014; Oke et al., 2019). The remaining portion of the EAC continues to flow south along the coast as part of the EAC southern extension generating a large eddy field (Everett et al., 2012). Along the continental shelf, particularly where the continental shelf narrows, the EAC has significant impact on shelf circulation (Schaeffer & Roughan, 2015). Current driven bottom friction leads to Ekman transport in the bottom boundary layer, moving cooler denser water up the slope, resulting in uplift of isotherms and upwelling (Schaeffer et al., 2014). These intrusion events have been shown to bring nutrient rich water into the euphotic zone, increasing nitrate (Rossi et al., 2014) and chlorophyll *a* concentration (Everett et al., 2014), and controlling vertical phytoplankton abundance and composition (Armbrecht et al., 2014, 2015). These EAC-driven upwelling or uplift events vary latitudinally rather than seasonally. Using a monthly climatology of altimetry over 12 years, Rossi et al. (2014) showed that the occurrence of these events is relatively consistent all year long north of the EAC separation ≈32°S, and quite rare further south. Wind driven upwelling can also occur with winds from the northeast favoring upwelling and winds from the southeast favoring downwelling (Wood et al., 2012). The typical euphotic depth in these waters is ≈50 m (Rocha et al., 2019).

From 2nd to 13th September 2004, a research voyage on the RV Southern Surveyor was undertaken from Sydney, Australia (33.82°S, 151.29°E) to Brisbane, Australia (27.36°S, 153.17°E). During this period, the EAC was flowing southward along the coast until approximately 31°S where it separated from the mainland and continued flowing to the east. This separation resulted in the formation of a large warm-core eddy forming off the coast at approximately 33°S, 155°E (Figure 1 and Figure S1 in Supporting Information S1), which is a common circulation in the area, irrespective of the month (Oke et al., 2019). The observed chlorophyll *a* levels in the area are also typical of those observed in September (Everett et al., 2014).

To investigate environmental conditions leading up to and during the sampling of transects on the east Australian continental shelf, MODIS-Aqua Level 3 ocean-color data (chlorophyll *a*) were obtained from the Integrated Marine Observing System (IMOS) Data Portal (http://imos.aodn.org.au/imos/) at 1 km resolution. Chlorophyll *a* was derived using the OC3 algorithm. Sea-surface temperature was obtained from L3S AVHRR daily night product from the same portal, displayed as a map for the region (resolution of 0.02°). Surface geostrophic currents were derived from gridded sea level gradients from satellite altimetry, also taking into account sea level gauges to improve estimates in coastal areas (resolution of 0.2°).

To investigate the seasonal variation of EAC strength in the region of our transects, 10 years (2004–2013) of surface geostrophic currents from satellite altimetry were obtained from the IMOS Data Portal (http://imos.aodn.org.au/imos/) for each of our transects. Alongshore and cross-shelf velocity of currents was calculated by rotating the U and V vectors to account for the angle of the coastline at each location (Table 1). The monthly mean (and standard deviation) alongshore velocity was calculated for the 10-year period by averaging the daily velocities. We assumed that faster alongshore velocity would be due to increased influence of the EAC which is known to seasonally widen, extending its influence over the continental shelf (Archer et al., 2017). Seasonal variation in surface chlorophyll *a* in this region was extensively investigated in Everett et al. (2014) based upon satellite data and showed that the chlorophyll *a* values observed in our study are typical of the region (within 1 SD of the geometric mean chlorophyll *a* values).

The potential influence of wind driven upwelling was investigated using wind data from Coffs Harbor meteorological station from the Bureau of Meteorology (30.311°S, 153.118°E) located close to shore at 5 m height (wind from the northeast is conductive to upwelling). The hourly wind stress was calculated following Wood et al. (2012). Bathymetric data were sourced from GEBCO (GEBCO Bathymetric Compilation Group, 2019).

Table 1
Summary of the Four Transects Undertaken Using the SeaSoar With Attached OPC and CTD

Transect	Coastline angle (°)	Start longitude (°E)	Start latitude (°S)	End longitude (°E)	End latitude (°S)	Start time	End time
Cape Byron	356	153.704	28.633	153.981	28.633	12 September 2004 08:11	12 September 2004 09:59
Evans Head	13	153.611	28.997	153.858	29.002	11 September 2004 10:55	11 September 2004 12:36
North Solitary	15	153.412	29.998	153.726	29.997	7 September 2004 21:41	8 September 2004 00:05
Diamond Head	19	152.913	31.752	153.191	31.747	6 September 2004 20:00	6 September 2004 21:53

Note. Times are local, Australian Eastern Standard Time (GMT +10). Cape Byron and Evans Head were conducted in daylight while North Solitary and Diamond Head were conducted at night.

2.2. Sampling

Four transects were sampled roughly perpendicular to the coast over a 7-day period (6–12 September; Table 1 and Figure 1) using a modified SeaSoar. The SeaSoar was towed from inshore to offshore and undulated between

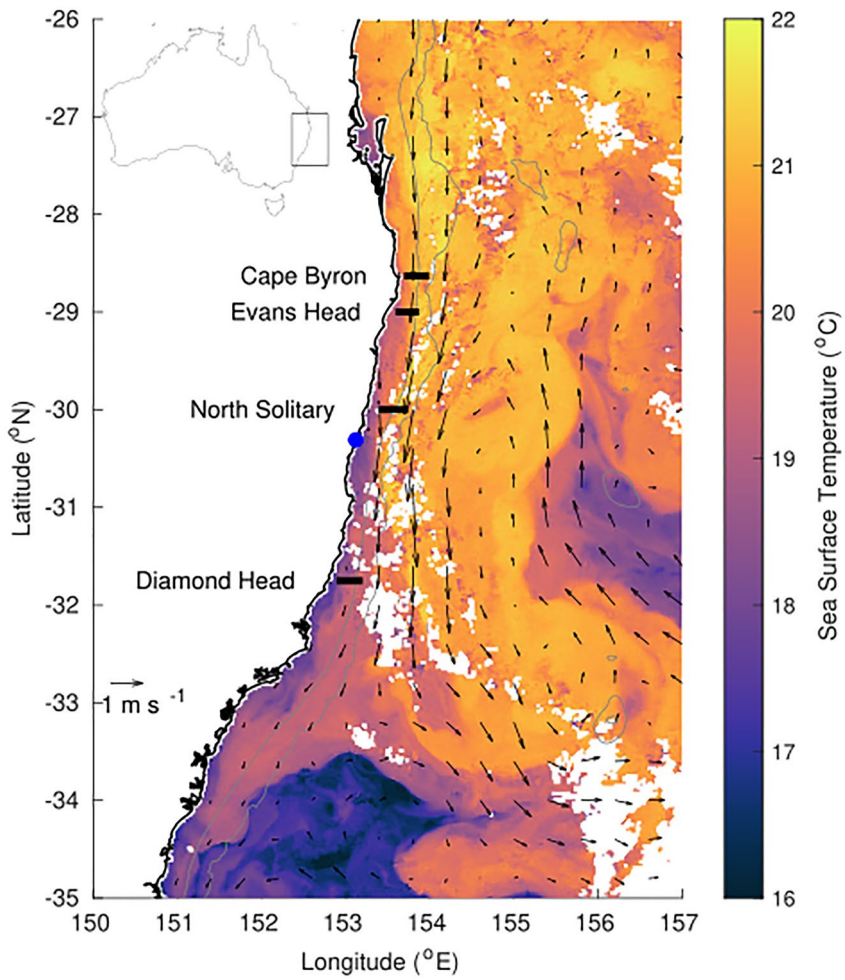

Figure 1. Locations of the four cross-shelf sections which were sampled in September 2004. The sea-surface temperature for 6 September 2004 is shown in color with velocity arrows from satellite altimetry shown with black arrows. Gray isobaths represent 200 and 2,000 m depths. The blue dot represents the weather station (Coffs Harbor) used for the upwelling calculations.

10 and 120 m depth as in previous studies (Baird et al., 2008). Mounted on the SeaSoar was a dual CTD system (custom made interface combining a Seabird SBE3 temperature sensor, a Seabird SBE4 conductivity sensor and a Paroscientific 43K-027 pressure sensor) and an OPC (Herman, 1992) to continuously measure temperature, salinity and the size frequency distribution of particles in the water column. An Acoustic Doppler Current Profiler (ADCP; Teledyne R. D. Instruments, USA, Model # VM-150) continuously monitored the current velocity profile beneath the vessel. Alongshore and cross-shelf velocity of currents were calculated using the same method as the satellite altimetry data, by rotating the U and V vectors to account for the angle of the coastline at each location (Table 1). Immediately following each SeaSoar deployments a transect of CTD deployments were conducted over the same course (in the opposite direction) to characterize nutrients, oxygen, and fluorescence along each transect. Fluorescence, temperature, salinity, and oxygen were electronically measured, while nutrients (nitrate NO_3^-, phosphate PO_4^{3-}, silicate $Si(OH)_4$) and oxygen samples were taken at the surface and depths of 25, 50, 75, 100, 150, and 200 m (unless shallower). Nutrient analysis followed techniques described in Cowley (1999) and has an approximate accuracy of 0.02 µM. Chlorophyll *a* was calculated as per Baird et al. (2008) following the method of Jeffrey and Humphrey (1975). Using surface samples ($n = 24$), calibration of the CTD fluorometer showed Chlorophyll $a = 0.0157(\text{Fluorescence}) + 0.4421$ ($r^2 = 0.53$).

2.3. Particulate Size Structure

The OPC was a Focal Technologies Corporation Model OPC-2T with a sampling aperture of 2 × 10 cm (Herman, 1992). The OPC records ESD of particles that pass through the instrument in 0.5 s intervals (Baird et al., 2008; e.g., Suthers et al., 2006). The particle sizes were recorded digitally using 4,096 size bins, corresponding within the operating range of the instrument to bins with a width varying between 5 and 15 µm. The particles used in the following analysis were restricted to those above 250 µm ESD to account for the lower detection limit of the OPC (Suthers et al., 2006).

The volume of flow through the sample region was based on distance measured over a 6 s interval. It has been previously shown that a 6 s interval provides optimal vertical and horizontal resolutions (≈6 m vertically) of the size distribution in the Tasman Sea region, near the current study area (Baird et al., 2008). To quantify the particulate size structure, several metrics were calculated for each interval of our transects (Krupica et al., 2012). These included total biomass (mg m^{-3}), geometric mean size (GSM; µm ESD) and zooplankton size spectrum slope which we calculated as the shape parameter *c* of the Pareto distribution of the particles (equivalent to the traditional NBSS slope). The OPC records the time and size of each particle detected, allowing the Pareto distribution to be calculated without further binning of the raw digital signal that is necessary for the NBSS. The correlation between the more common NBSS Slope and shape parameter *c* of the Pareto distribution was also tested to confirm the relationship. The Pareto distribution has been previously used in this region to spatially resolve the size distribution of particles (Baird et al., 2008; Suthers et al., 2006).

The Pareto distribution has a probability density function (*pdf*) defined as:

$$pdf(s) = ck^c s^{-(c+1)}$$

where *s* is the size of the particle, and *c* and *k* are the distribution's shape and scale parameters, respectively (Vidondo et al., 1997). ESD values (µm) were converted to biomass (wet weight; mg m^{-3}) as per Wallis et al. (2016), assuming the volume of a sphere and the density of water ($\rho = 10^9$ mg m^{-3}) using:

$$\text{Biomass}\left(\text{mg m}^{-3}\right) = \frac{4}{3}\pi\left(\frac{\text{ESD}}{2}\right)^3\rho$$

Under our assumption that our particles have the density of water, 1 mg is therefore equivalent to 1 mm^3, resulting in our Biomass $\left(\text{mg m}^{-3}\right)$ being equivalent to the often reported biovolume (mm^3 m^{-3}) and we have labeled our plot axes as such. Particulate data from the OPC were interpolated to create 2D visualizations of the profiles across the continental shelf using the "akima" R package to interpolate a regular grid of points via bivariate interpolation (Akima & Gebhardt, 2020), then applying contours within the "ggplot" package (Wickham, 2011) within R v4.0.2 (R Core Team, 2020).

When interpreting size spectra metrics, particularly those involving mesozooplankton (the size range investigated in this study; generally primary and secondary consumers), higher primary production and biomass tends to

result in a higher elevation (or intercept of the NBSS) with such impacts demonstrated with nutrient input in both estuarine and pelagic ecosystems (Baird et al., 2008; Moore & Suthers, 2006). Steeper slopes in the size spectrum represent inefficient energy transfer between trophic levels which can occur under both oligotrophic conditions as nutrients become scarce and eutrophic conditions as many bloom taxa are relatively large yet unpalatable which increases the chances of mass sinking of ungrazed blooms leading to reduced efficiency of energy transfer (Atkinson et al., 2021). Top-down pressure from larger predators can also increase the steepness of the size spectrum as the mortality rates of the zooplankton increase, thereby decreasing the efficiency of energy transfer along the spectrum (Moore & Suthers, 2006; Rossberg et al., 2019).

The results from each OPC transect were categorized based upon both oceanographic water mass and depth. Based upon natural breakpoints (as observed in the visuals of the transects), we observed in the transect isotherms, we defined waters warmer than 21°C as core EAC water, water <20°C as Tasman Sea water (representing both Tasman Sea water and cool upwelled water from below the core EAC) and water between 20 and 21°C as frontal water. To highlight patterns with depth we also separated the OPC results into <25, 25–50, and >50 m bins. We calculated the mean biomass, abundance, size spectrum slope, and GMS for each of these water mass and depth combinations (Table S2 in Supporting Information S1). To qualitatively assess any impact of diel vertical migration, we compare OPC results in each depth bin for core EAC water (offshore waters) from the Cape Byron (day sample), Evans Head (day sample), and North Solitary (night sample) using boxplots to see if there are noticeable differences in vertical distribution of particles.

2.4. A Global Context

To place our east Australian transects in a global context and identify general trends in zooplankton size structure on continental shelves, we examined 20 previous studies which investigated spatial changes in zooplankton communities over continental shelf regions. While each continental shelf is unique and the ecological and environmental context of each study will differ, nutrient enrichment is common among all continental shelves. This enrichment comes from a variety of sources including upwelling (Malan et al., 2020; Roughan & Middleton, 2002), run-off (Correll et al., 1992), and estuarine processes (Morris et al., 1995) but for the context of our global comparison we are only concerned with the resulting pattern of zooplankton or particles across the continental shelves. Where possible from each study we extracted values for total biomass (or biovolume (m^{-3})), abundance (m^{-3}) and the size spectrum slope from the most inshore and furthest offshore sites (Table S3 in Supporting Information S1). From each study we extracted one inshore and one offshore value, averaged across the study as well as corresponding bathymetry values, except for two studies from the Bay of Biscay (Irigoien et al., 2009; Vandromme et al., 2014), where the east and south regions had very different zooplankton communities so they were kept as distinct regions. If there were multiple years or seasons within a study, an average was taken. In the case of our samples, we took the average of the endpoints of all four of our transects. As many studies only provided binned values or plots, data were estimated from plots using a color sampling tool and binned data were assigned values equal to the midpoint of the bin (Table S3 in Supporting Information S1). As the studies reported a range of units, to make studies comparable in terms of inshore to offshore trends we present the ratio of inshore to offshore values.

As an additional analysis, we repeated the abundance and biomass ratio calculations using zooplankton depth integrated metrics calculated using m^{-2} rather than m^{-3}. This provides a different, wholistic view of the zooplankton community in the whole column. The m^{-2} metrics were calculated by multiplying the m^{-3} values by the bathymetry or 200 m (whichever was shallower). This allows us to compare only the water at continental shelf depths.

3. Results

3.1. Regional Oceanography and Seasonality

At the time of our sampling, the three northern most transects (north of 30°S) all crossed from cooler inshore waters into warm EAC water contrasting the southern transect (Diamond Head 31.75°S), which was located south of where the EAC begins to separate from the shelf ("the separation zone"; Figure 1). All transects showed low chlorophyll *a* levels (<1.4 mg m^{-3}; Figure S1 in Supporting Information S1). Most transects were negligibly influenced by the effects of wind in the 3 days prior to the transects, with most of the wind coming from a

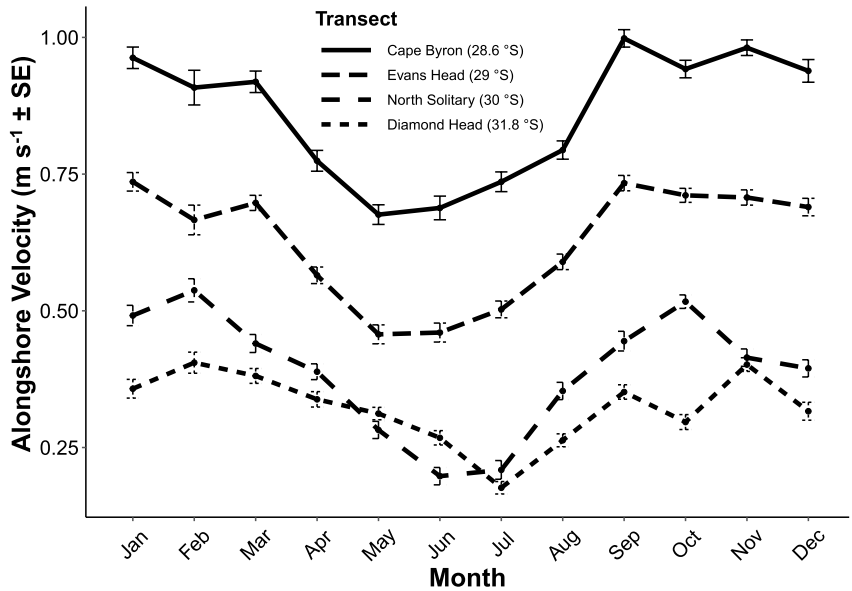

Figure 2. Seasonal changes in mean alongshore surface velocity (mean m s^{-1} with standard error (SE); toward ~195°, minor variation in coastline angle between sites) at the Cape Byron (28.6°S), Evans Head (29°S), North Solitary Island (30°S), and Diamond Head (31.8°S) based upon 10 years of satellite altimetry data (2004–2013). Velocity data were downloaded for the eastern edge of each transect (Table 1) from the IMOS Data Portal (http://imos.aodn.org.au/imos/). The EAC separates from the coastline between approximately 28°S and 32°S (Cetina-Heredia et al., 2014). The alongshore flow is in an approximate southerly direction.

southerly direction. The exception was the North Solitary (30°S) transect which was subject to some wind driven upwelling prior to our sampling (Figure S2 in Supporting Information S1).

In terms of seasonality, satellite altimetry showed alongshore velocity varies at our transects throughout the year by approximately 0.25 m s^{-1}, with the northern sites having the fastest overall flow (Figure 2). The alongshore velocity at all sites was reduced between April and August before increasing in spring (when our observations were taken) and summer. This seasonality is consistent with previous findings from higher-resolution HF radar observations around 30°S (Archer et al., 2017). Despite the seasonality in EAC speed, the main factor is latitude, with mean monthly velocities greater than 0.45 m s^{-1} all year round north of 30°S (Cape Byron 28.6°S annual mean velocity 0.86 m s^{-1} (0.30 SD), Evans Head 29°S annual mean velocity 0.63 m s^{-1} (0.25 SD)), compared to the Diamond Head site (31.8°S), where they rarely reach that magnitude (Figure 2; annual mean velocity 0.32 m s^{-1} (0.21 SD)). Therefore, we expect the observed cross-shelf gradients in water masses (temperature, salinity) induced by the EAC in the northern sites to be consistent all year round.

3.2. Potential Impact of Diel Vertical Migration

Comparing the OPC particle results across depth bins for the day (Cape Byron, Evans Head) and night (North Solitary) transects in core EAC waters revealed no shifts in the depth resolved patterns of biomass, abundance, GMS or the Pareto shape parameter. The depth patterns seen during the night transect matched at least one of the day transects for all OPC parameters (Figure S3 in Supporting Information S1). This suggests that diel vertical migration is not a major factor influencing the patterns observed in this study.

3.2.1. Cape Byron (28.6°S)

The northernmost transect at Cape Byron (28.6°S) was dominated by the EAC which had a strong alongshore flow (1.50 m s^{-1}; Figure 3) and weak cross-shelf flow (0.1–0.2 m s^{-1} toward the coast; Figure S4 in Supporting Information S1). The EAC was centered 27.6 km offshore, above the 200 m isobath. Most of the continental shelf was flooded by warm EAC water (see isotherms in Figure 4). There was evidence of uplift with the 21°C isotherm rising to the surface from 70 m depth over 5 km and the 20°C isotherm rising to the surface from 100 m depth over 15 km (Figure 4). Due to the proximity of the strong EAC from the continental slope (Figure 3) and the lack

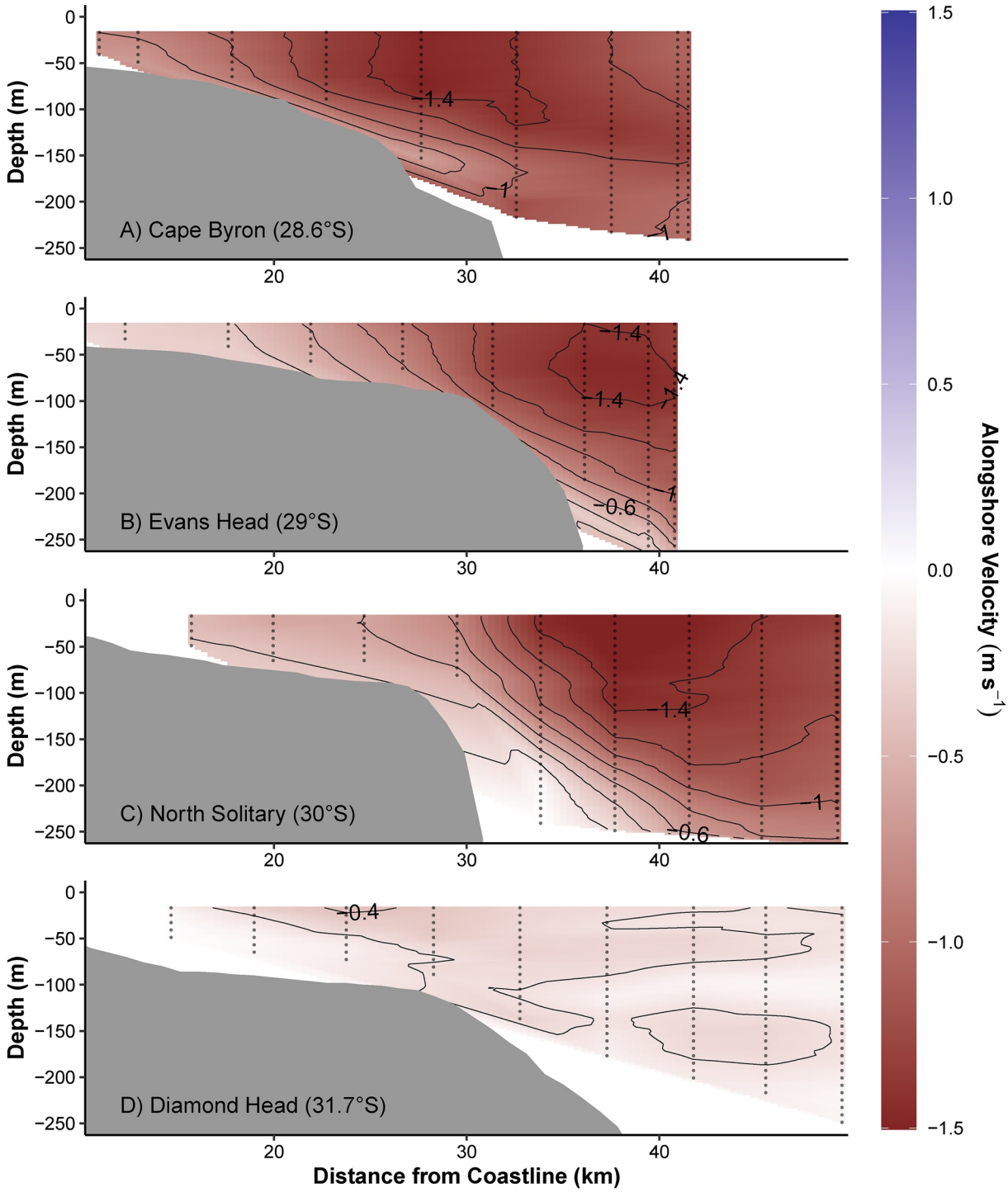

Figure 3. Alongshore (toward ~195°, minor variation in coastline angle between sites) velocity across the four cross-shelf transects (Figure 1), from the vessel's Acoustic Doppler Current Profiler. Gray lines join areas of equal velocity.

of upwelling-favorable wind stress (Figure S2 in Supporting Information S1), the isotherm uplift is likely to be current driven, hence driven by the strong bottom stress induced by the EAC, as shown in Schaeffer et al. (2014).

A decline in particulate biomass and abundance was observed from both inshore to offshore and from the surface to depth with the highest biomass (~750 mg m^{-3}; Figure 4 and Figures S5–S7 in Supporting Information S1) observed in the top 50 m ≈ 20 km from the coastline, just inshore of the 21°C isotherm in the frontal water

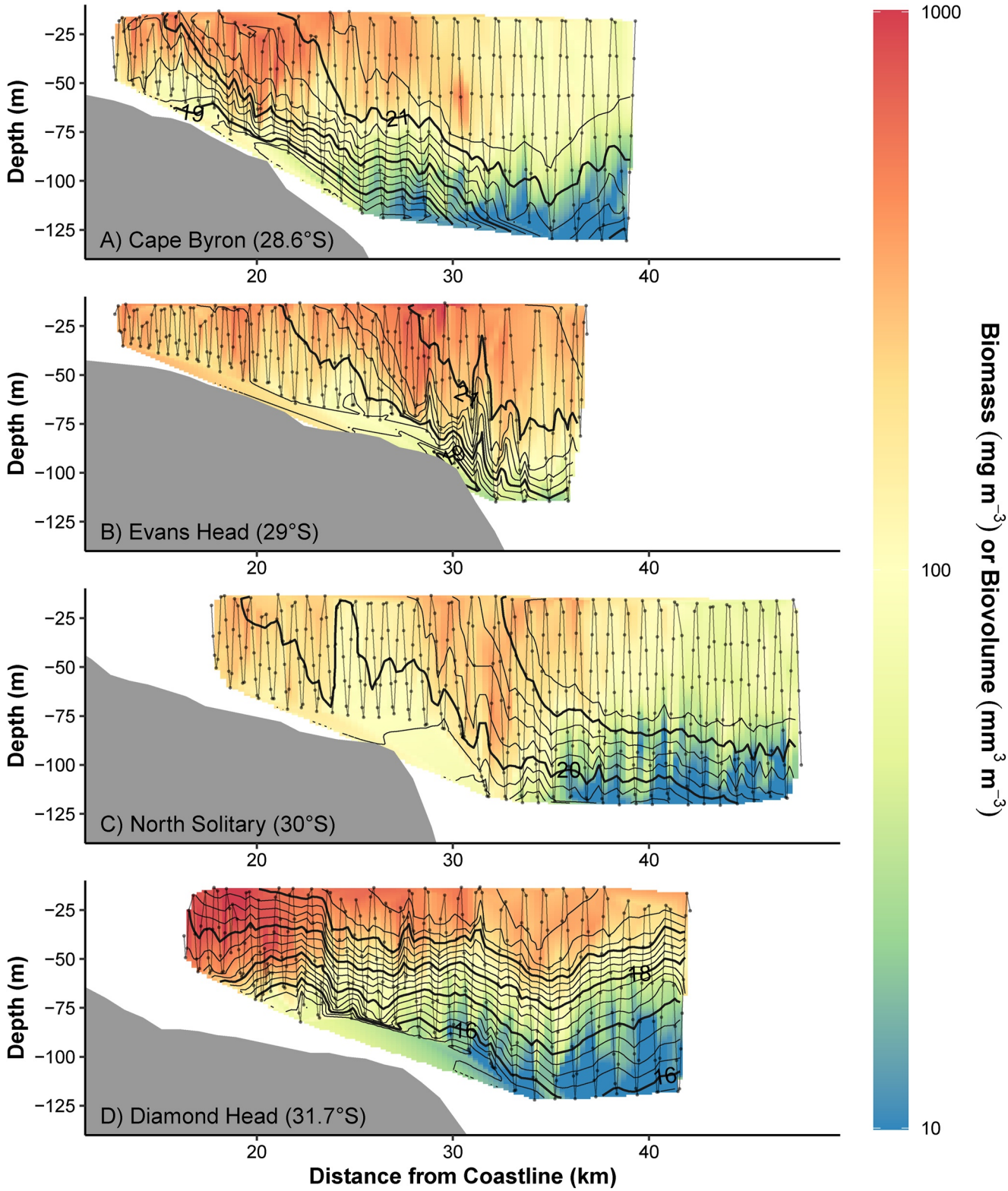

Figure 4. Particulate biomass (mg m^{-3}) or biovolume (mm m^{-3}) distributions from the four cross-shelf transects (Figure 1). Transects were conducted from inshore to offshore with an undulating towed body with the path shown by the gray line with midpoints of each sample shown as dots. Temperature (°C) isotherms are shown in black. Note the $\log_{10}$ transformed color scale.

(Figure 4 and Table S2 in Supporting Information S1). The warmer offshore EAC waters were characterized by lower biomass with a GMS of ≈450 μm ESD (Figure 5 and Table S2 in Supporting Information S1) with steep size spectrum slopes between −1 and −1.3 (Figure 6). The frontal water immediately inshore of the 21°C isotherm had high biomass and a shallower size spectrum slope (−0.9; Figures 4 and 6) with larger particles (GMS 500 μm ESD; Figure 5 and Table S2 in Supporting Information S1). Further inshore again (15–17 km from the coastline), in water <20°C, biomass remained high (Figure 4), but the particles were smaller (GMS ≈ 430 μm ESD; Figure 5 and Table S2 in Supporting Information S1), resulting in a steeper size spectrum slope (≈−1.25; Figure 6). No depth resolved cross-shelf chlorophyll *a* or nutrient data was available for the Cape Byron transect but there was a gradient in both salinity and temperature across the shelf. Warmer saltier water was found in offshore water, with the salinity both showing similar uplift onto the shelf as described above for the temperature isotherms (Figure S8 in Supporting Information S1).

3.2.2. Evans Head (29°S)

The transect at Evans Head (29°S) extended only 5 km past the continental shelf edge but was still largely influenced by the EAC. The EAC was centered 36.1 km from the coast above the 220 m contour. The EAC had a strong alongshore flow (1.47 m s^{-1}; Figure 3). The EAC showed offshore movement (0.27 m s^{-1}) which increased with distance offshore (Figure S4 in Supporting Information S1). There was strong uplift of the isotherms inshore of the EAC with the 21°C isotherm rising to the surface from 70 m depth over 6 km and the 20°C isotherm rising to the surface from 100 m depth over 15 km (Figure 4), closely aligned with the contours of the EAC southward velocity (−0.8 m s^{-1}). This uplift created a small frontal zone between the cooler inshore/deeper water and the warmer offshore EAC. The fast EAC encroaches the bottom of the continental shelf as in Cape Byron transect, most likely driving the isotherms uplift in a similar way to Diamond head (as demonstrated in Schaeffer et al. (2014)). Note that wind stress at the time was not particularly upwelling favorable (Figure S2 in Supporting Information S1).

The particulate size structure varied along the transect. The EAC was warmer and saltier compared to the inner shelf water (Figure S8 in Supporting Information S1). There was also a slight gradient in nitrate and chlorophyll *a* with higher levels of both in the inshore waters (3 mmol m^{-3} and 1.35 mg m^{-3}, respectively; Figures S9 and S10 in Supporting Information S1). In the warmer offshore water, the biomass and GMS was similar to offshore at Cape Byron, while in the cool inshore waters, there was again high particulate biomass (Figure 4), but the community had shifted toward smaller particles which resulted in a more negative *c*, representing a steeper size spectrum slope (<−1.3; Figures 5, 6 and Table S2 in Supporting Information S1). There was a minor peak in biomass in the frontal zone between the water masses. There was also low abundance in the deeper samples (Figure S7 and Table S2 in Supporting Information S1).

3.2.3. North Solitary (30°S)

The transect at North Solitary (30°S) showed the strongest evidence of uplift of any of the transects with the 21°C isotherm rising to the surface from 70 m depth over 3 km and the 20°C isotherm rising to the surface from 100 m depth over 10 km (Figure 4). The EAC was centered 37.7 km offshore (alongshore flow 1.59 m s^{-1}), located above the 310 m bathymetry contour (Figure 3). This uplift could potentially have been influenced by the upwelling-favorable winds in the hours leading up to sampling (Figure S3 in Supporting Information S1), although we are not certain of the exact nature of the shoaling feature as it appeared to move east and the isotherms become steeper in the hours between the SeaSoar sampling and CTD transect (Figure S10 in Supporting Information S1). The offshore waters of the EAC showed slight onshore movement, at depths of 100–150 m (0.15 m s^{-1}; Figure S4 in Supporting Information S1).

Biomass and abundance generally decreased with distance offshore and with depth (Figure 4 and Figures S5–S7 in Supporting Information S1). The warmer core EAC water, located offshore, contained low biomass with a shallow pareto distribution shape parameter *c* (−0.9) and GMS of ≈450 μm (Figures 4–6 and Table S2 in Supporting Information S1). Particulates in cooler water <20°C had a much smaller GMS (≈410 μm ESD) correlating with a more negative *c*, representing a steeper size spectrum slope (<−1.3; Table S2 in Supporting Information S1). This was particularly evident in the frontal water where the 20°C isotherm reached the surface ≈24 km from the coastline, bringing to the surface upwelled water higher in nitrate, chlorophyll *a* and particles with a smaller mean size (Figure 5 and Figures S9, S10 in Supporting Information S1). Based on the upwelling-favorable wind a few hours before sampling, the uplift is possibly recent (although there may be upwelling contributed from the close

10.1029/2022JC018689

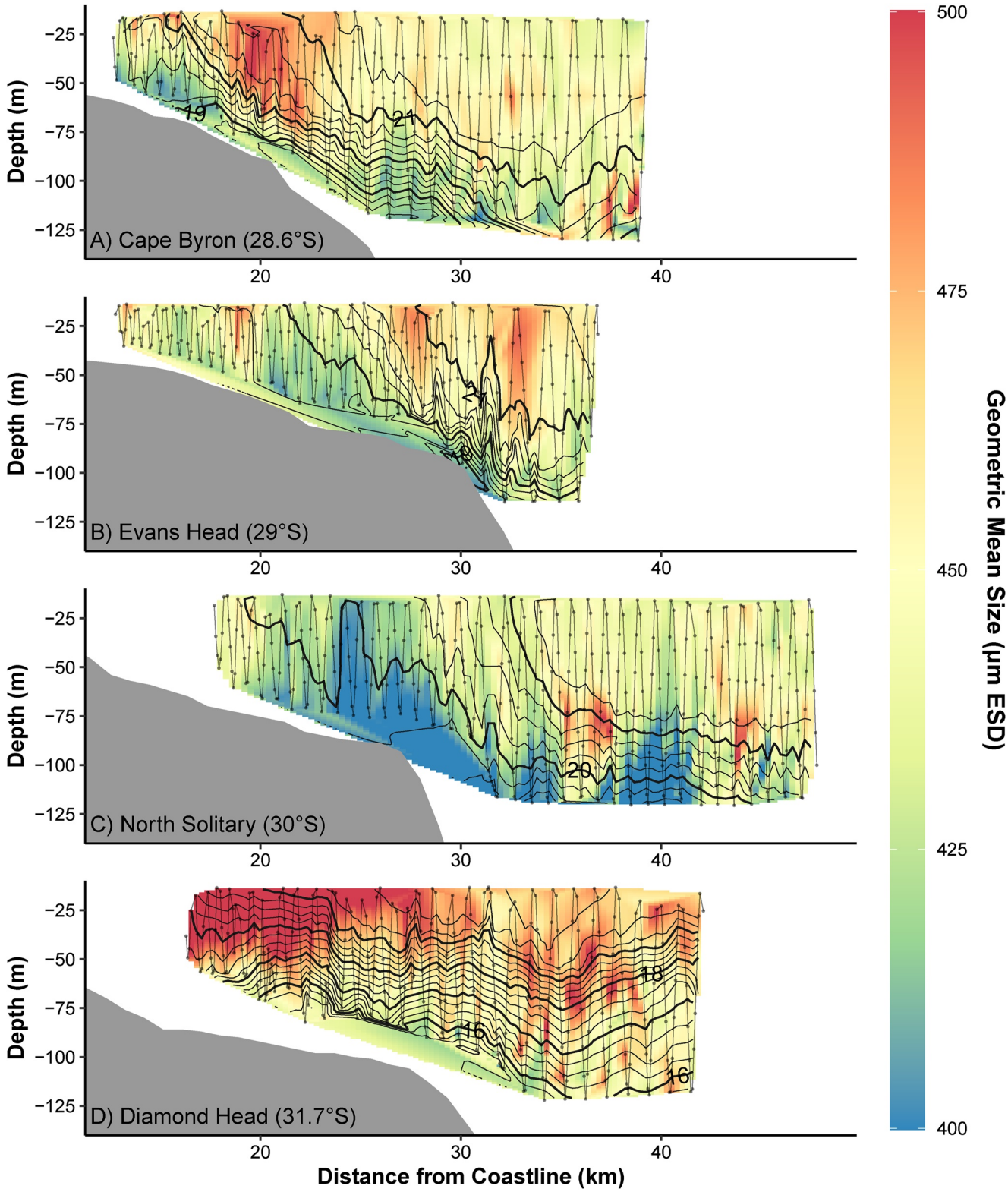

Figure 5. Geometric mean size (µm equivalent spherical diameter; ESD) of particulates from the four cross-shelf transects (Figure 1). Transects were conducted from inshore to offshore with an undulating towed body with the path shown by the gray line with midpoints of each sample shown as dots. Temperature (°C) isotherms are shown in black.

10.1029/2022JC018689

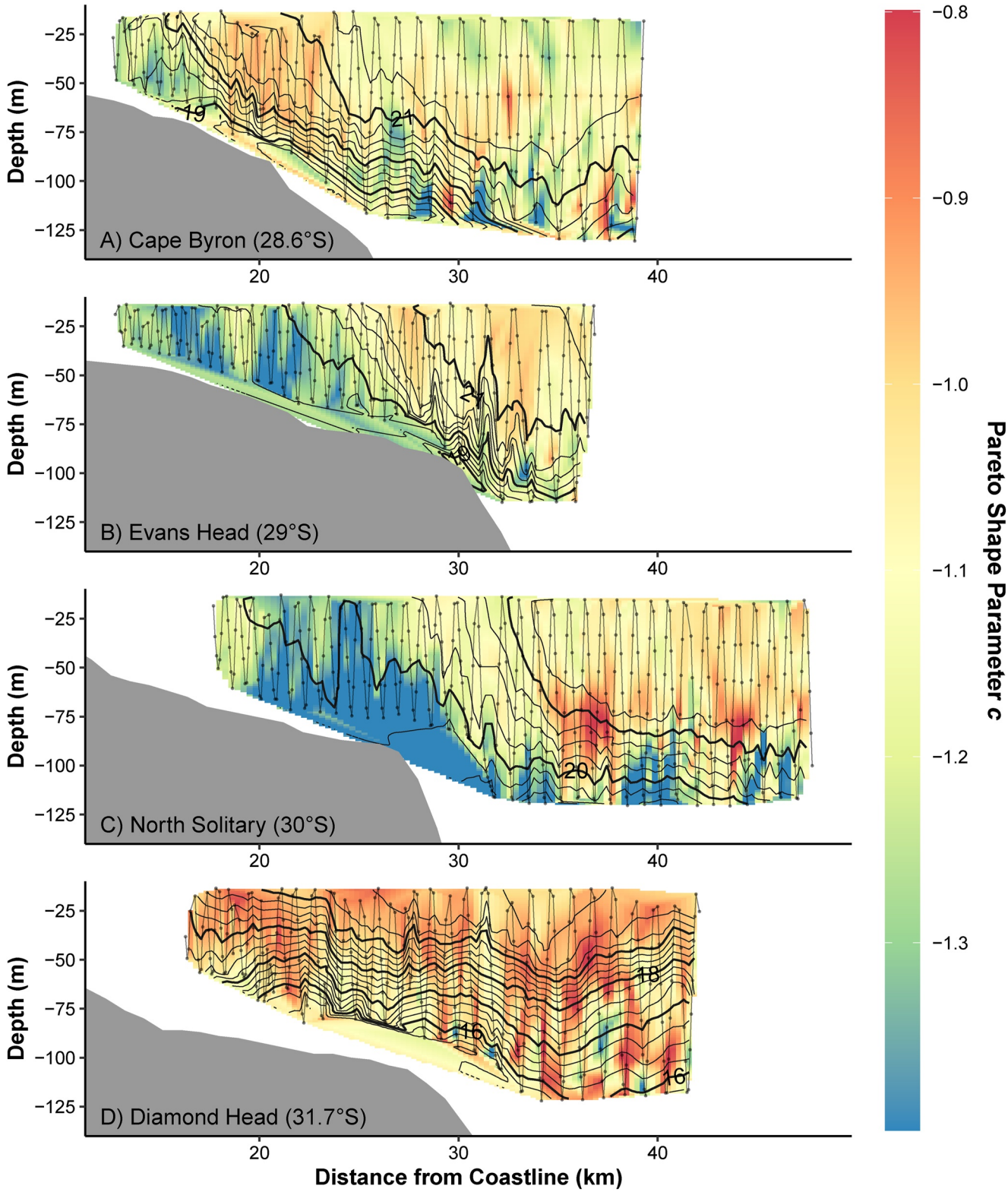

Figure 6. Interpolations of the shape parameter *c* from the Pareto distribution of particulate size from the four cross-shelf transects (Figure 1). This is a robust estimate of the normalized biomass size spectrum slope (shown in Figure S16 in Supporting Information S1). Transects were conducted from inshore to offshore with an undulating towed body with the path shown by the gray line with midpoints of each sample shown as dots. Temperature (°C) isotherms are shown in black.

EAC). This upwelled water had a lower biomass than surrounding water possibly because there has been no time for the nutrients and productive potential to flow into the larger mesozooplankton community.

3.2.4. Diamond Head (31.75°S)

The most southern transect located at Diamond Head (31.75°S) was not influenced by the EAC which had separated from the coast to the north and was characterized by a more homogeneous water mass consisting of Tasman Sea water. Here, the alongshore velocities were low (<0.43 m s^{-1}, Figure 3) with low onshore movement of water (0.11 m s^{-1}) in the surface waters and offshore movement (0.27 m s^{-1}) in the deeper waters (Figure S4 in Supporting Information S1). The lack of horizontal variation was reflected in the nitrate, silicate, temperature, and salinity with almost all variation being observed with depth (Figures S8, S11, and S13 in Supporting Information S1). Chlorophyll *a* and oxygen showed small peaks (1.2 mg m^{-3} and 240 mmol m^{-3}, respectively; Figures S12 and S14 in Supporting Information S1) at the surface near the beginning of the transect. There was minor uplift of the temperature isotherms with all isotherms rising approximately 20–40 m as they came onto the continental shelf. This uplift is likely caused by the separation of the EAC from the coast to the north, generating uplift through the creation of eddies near Diamond Head rather than current driven uplift observed at the northern EAC influenced sites (Roughan & Middleton, 2002; Schaeffer & Roughan, 2015).

This transect has the highest observed biomass of particles (>1,000 mg m^{-3}), particularly inshore (Figure 4 and Table S2 in Supporting Information S1). The size structure was not clearly related to water masses reflecting the more homogenous water mass here, not sampling EAC water. Inshore, the particulate community was charactered by larger individuals (GMS ~500 µm ESD; Figure 5) and had higher overall biomass which declined steadily with distance offshore and with depth (Figure 4 and Figures S5, S6, Table S2 in Supporting Information S1). The pareto distribution shape parameter *c* of the community was shallow over the whole transect (≈−0.9; Figure 6 and Table S2 in Supporting Information S1).

3.3. Synthesis of Transect Patterns

The influence of the EAC varied between the four transects. The three northern transects were influenced strongly by the EAC, particularly the offshore sections while the Diamond Head transect was not influenced by the EAC. At the two northern sites, the EAC was located close to the continental shelf and likely drove current driven upwelling. In contrast at the North Solitary site, the EAC was located further offshore, and the weaker observed uplift was potentially caused by wind driven upwelling (Figure S2 in Supporting Information S1).

The Cape Byron, North Solitary, and Diamond Head transects had higher particulate biomasses observed in continental shelf waters with declines offshore and with depth in the top 100 m of the water column (Figures S5 and S6 in Supporting Information S1). The decline with distance to coast held even when the analyses were restricted to samples taken in the top 50 m of the water column and the decline with depth in the water column was more pronounced when restricted to samples taken in areas of deeper bathymetry (>25 km offshore; Figures S5 and S6 in Supporting Information S1). The transect at Evans Head did not show a noticeable decline in biomass with distance from the coast instead it showed a peak in biomass in the frontal water between the cooler inner shelf water and the EAC water (Figure 4 and Table S2 in Supporting Information S1).

Three patterns in GMS were evident in our four transects. Cape Byron and to a lesser extent, Evans Head showed evidence of larger GMS around the front between the warm EAC and cooler inner shelf water (around the 21°C isotherm; Figure 5). North Solitary showed evidence of uplift with the small GMS community from deep uplifted to the surface. Diamond Head was different with a more homogenous distribution of GMS although there was a trend of larger particulates inshore. The size structure of all sites was related to the GMS with steeper size spectrum slopes in areas with smaller zooplankton (Figures 5 and 6). The Pareto shape parameter *c* was highly correlated with the NBSS Slope but provided better fewer gaps (due to low numbers of particles) over the transects ($r = 0.934$, $t_{535} = 60.362$, $p < 0.001$, Figure S13 in Supporting Information S1).

3.4. Global Synthesis

Twenty-one studies quantified the cross-shelf changes in mesozooplankton and/or particles (including this study), revealing a broad consensus (Figure 7 and Table S3 in Supporting Information S1), even though many studies were not influenced by a WBC. Nine studies (including ours) reported abundance values for inshore and offshore

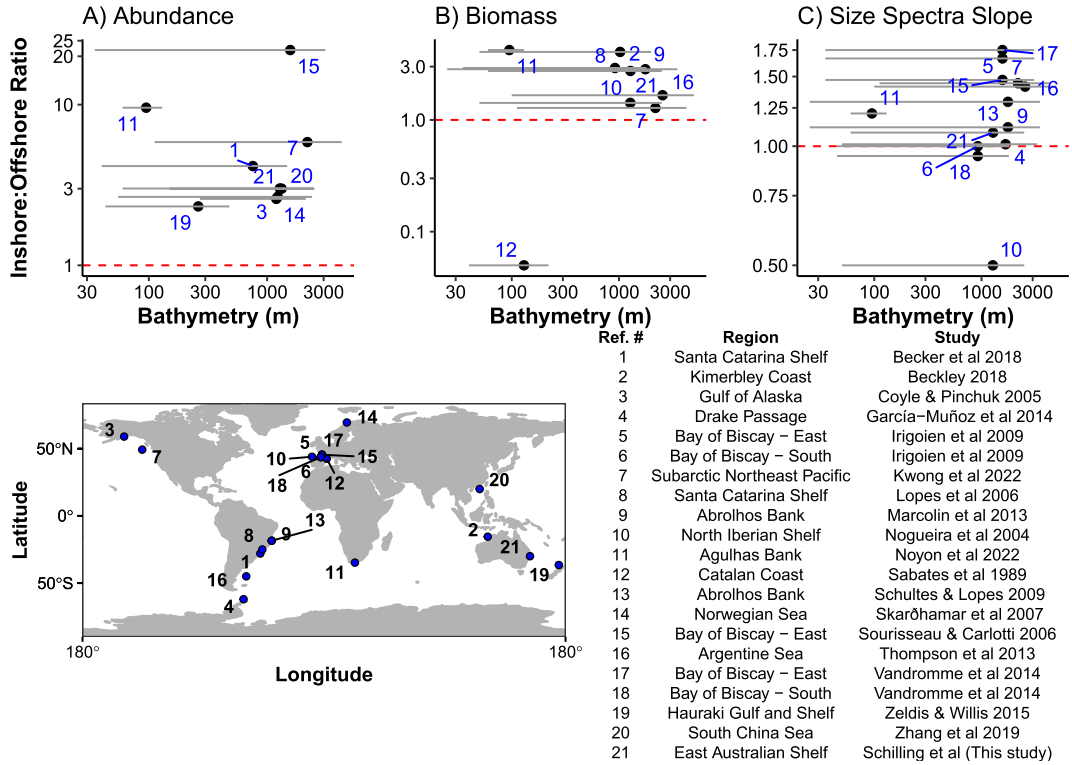

Ref. #	Region	Study
1	Santa Catarina Shelf	Becker et al 2018
2	Kimerbley Coast	Beckley 2018
3	Gulf of Alaska	Coyle & Pinchuk 2005
4	Drake Passage	García−Muñoz et al 2014
5	Bay of Biscay − East	Irigoien et al 2009
6	Bay of Biscay − South	Irigoien et al 2009
7	Subarctic Northeast Pacific	Kwong et al 2022
8	Santa Catarina Shelf	Lopes et al 2006
9	Abrolhos Bank	Marcolin et al 2013
10	North Iberian Shelf	Nogueira et al 2004
11	Agulhas Bank	Noyon et al 2022
12	Catalan Coast	Sabates et al 1989
13	Abrolhos Bank	Schultes & Lopes 2009
14	Norwegian Sea	Skarðhamar et al 2007
15	Bay of Biscay − East	Sourisseau & Carlotti 2006
16	Argentine Sea	Thompson et al 2013
17	Bay of Biscay − East	Vandromme et al 2014
18	Bay of Biscay − South	Vandromme et al 2014
19	Hauraki Gulf and Shelf	Zeldis & Willis 2015
20	South China Sea	Zhang et al 2019
21	East Australian Shelf	Schilling et al (This study)

Figure 7. Summary of previous studies investigating cross-shelf patterns of mesozooplankton and/or particles (#21 is the current study). The *y* axis shows the ratio of the inshore to offshore reported values for zooplankton (a) abundance, (b) biomass, and (c) the size spectrum slopes. A ratio greater than 1 (red dashed line) means that the inshore region had a larger abundance/biomass or steeper size spectrum. Each numbered dot represents a study except for the studies in the Bay of Biscay which identified east and south as distinct region so they remain independent (Table S3; Irigoien et al., 2009; Vandromme et al., 2014). The *x* axis represents the bathymetry range from each study with the dot on the mean value for that study. Note the $\log_{10}$ axes. Of the studies, #'s 3, 4, 5, 6, 16, 19, and 20 made an attempt to only analyze true zooplankton particles while all other studies analyzed a combination of pelagic particles (as in the current study).

and all found that abundance was higher in inshore regions compared to offshore regions. Eight of these studies showed inshore areas abundance of 2.3–9.6 times higher than offshore values with one study from the eastern Bay of Biscay region finding a 22-fold difference (Sourisseau & Carlotti, 2006). For biomass, eight of nine studies showed 1.2–4.2-fold greater biomass inshore compared with offshore (Figure 7 and Table S3 in Supporting Information S1). The ninth study (from the Western Mediterranean) showed 20-fold higher biomass offshore compared to inshore values (Sabatès et al., 1989).

In terms of size structure, 13 studies reported both inshore and offshore values with 11 (including the current study) finding steeper zooplankton size spectrum slopes in inshore areas compared with offshore areas (Figure 7 and Table S3 in Supporting Information S1). The southern Bay of Biscay and North Iberian Shelf studies were unusual in having a shallower inshore zooplankton size spectrum slope compared to the offshore areas (Nogueira et al., 2004; Vandromme et al., 2014). It should be noted these analyses used averages of all transects in each study and in our case, one of 4 transects (Diamond Head) did not show this clear inshore-offshore pattern.

When the analysis was repeated using m^{-2} zooplankton metrics for abundance and biomass, the inshore-offshore gradients largely disappeared (Figure S14 in Supporting Information S1). There was no consistency in abundance gradients with four out of nine studies showing higher abundance per m^2 inshore. Only two out of nine studies showed a higher biomass per m^{-2} inshore.

4. Discussion

The size spectrum of particulate communities provides important information about the transfer of energy from phytoplankton to fish, from which we can understand how higher trophic levels including fisheries are supported

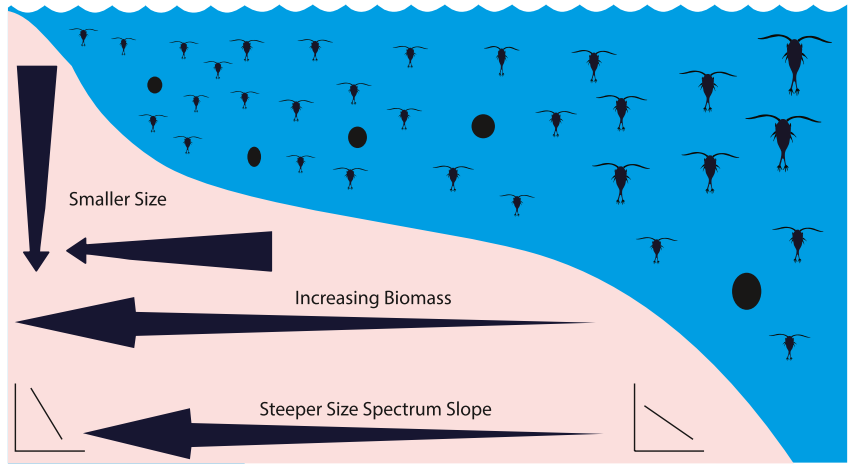

Figure 8. Conceptual diagram of the particulate community and how it changes over the east Australian continental shelf and with depth (to 100 m depth). Note the ratio of plankton (represented by copepods here) to other particulates (black ellipses here) is not representative.

on continental shelves. We found consistent declines from inshore to offshore in particulate biomass and variation in size structure both horizontally and vertically across the narrow continental shelf off eastern Australia (Figure 8). These horizontal trends in the particulate size structure are consistent with the patterns in size structure across other continental shelves and likely are an outcome of nutrient enrichment which tends to occur on continental shelves. This enrichment can come from a variety of sources including cross-shelf flows and sporadic upwelling processes driven by ocean currents and coastal winds (Malan et al., 2020; Rossi et al., 2014; Roughan & Middleton, 2002), estuarine process (Morris et al., 1995) or run-off from land (Correll et al., 1992).

4.1. Effects of the EAC on the Particulate Community

The separation of the EAC from the Australian coast, where it often bifurcates toward the east, forms a front between the northern oligotrophic waters, and the southern eutrophic Tasman Sea waters (Oke et al., 2019). Offshore, this can separate distinct particulate size structures (Baird et al., 2008). These distinct size structures can influence the abundance and diet of fish (Hobday & Hartmann, 2006; Revill et al., 2009). We observed similar differences in the particulate communities between water masses in the cooler inner shelf/Tasman Sea water and the warm EAC water. Our results suggest that the three northern transects are strongly influenced by the EAC whereby the continental shelf waters are, to a small extent influenced by uplift of deep nutrient rich water mostly driven by the close proximity of the EAC to the continental shelf (Roughan & Middleton, 2002; Schaeffer et al., 2014). The uplift likely drives the higher biomass of phytoplankton (Everett et al., 2014) which can flow into zooplankton (a key component of the particulate community we quantified). It should be noted that phytoplankton and zooplankton blooms rarely occur concurrently and sometimes within a single study it is possible that only phytoplankton or zooplankton may be high due to the differences in turnover periods. We observed a higher biomass and steeper size spectrum particulate community inshore of the EAC (in the cool inshore water prior to the frontal zone which sometimes showed a shallow slope) compared to the offshore EAC water, consistent with observations from some areas of other WBCs such as the Agulhas Current where biomass was higher inshore in the central Agulhas Bank but not the eastern region while the size spectrum slope was steeper inshore across the whole area (Noyon et al., 2022).

Closer inshore over the shallow bathymetry, it is possible predation pressure from fish in the littoral zone, particularly on temperate reefs, may remove certain size classes (usually larger) of plankton (Holland et al., 2020, 2021; Schilling et al., 2022; Truong et al., 2017), as has been shown on smaller scales previously (Hamner et al., 1988). A steeper zooplankton size spectrum slope in the cooler inner shelf waters could therefore arise not only from increased production of smaller zooplankton (Guiet et al., 2016), but also by predation on larger zooplankton prey by planktivorous fish (Moore & Suthers, 2006).

In contrast to the northern transects, the southern transect (Diamond Head; 31.75°S) was south of the EAC separation zone and only had Tasman Sea water with no EAC presence, resulting in larger particles and a shallower

size spectrum slope overall. The same pattern of decreasing biomass offshore, and with depth in the water column occurred despite only having a single water mass. As expected, the Tasman Sea has an elevated nutrient concentration and higher particulate biomass compared to the oligotrophic EAC waters (Baird et al., 2008). This was observed in our northern surveys to a limited extent with the EAC showing very small nutrient concentrations compared to the deeper and inner shelf waters (Figures S9 and S11 in Supporting Information S1). At our southern site there are two possibilities for this cross-shelf gradient. First, as there was no EAC influence at the southern site it is possible that the zooplankton are being retained on the continental shelf in this location due to weak flow in the lee of the EAC separation (Everett et al., 2014; Schaeffer & Roughan, 2015). Second, this region has been shown to have high chlorophyll a production due to both wind driven and current driven upwelling reliably generating increases in chlorophyll a (Everett et al., 2014). Regional climatology of chlorophyll a shows consistently higher chlorophyll a values at the southern transect (Everett et al., 2014). The consistency of this pattern in chlorophyll a suggests that these trends in production may be persistent enough to flow through into the zooplankton community. Consistent enrichment (or retainment) would naturally result in a higher biomass and size spectrum intercept, but the slope of the size spectrum would depend on mechanisms driven by trophic transfer of biomass. We observed a steeper inshore size spectrum at all sites (except Diamond Head) and believe this is likely due to inefficient transfer of biomass into the larger organisms (a mechanism demonstrated by Atkinson et al. (2021)). Although it is also possible the steeper slope may have come from high predation pressure as discussed above.

Across three of our transects there was a distinct frontal zone between the cooler inshore water and warmer EAC water. In this frontal zone there was generally a higher biomass compared to the inshore and EAC water masses, disrupting the inshore-offshore gradient (Table S2 in Supporting Information S1). While not a focus of the current study, these frontal regions are extremely interesting and further investigation of them is deserved, particularly more modern high-resolution sampling tools such as the "triaxis" or other moving vessel profilers which may better resolve features such as vertical velocities (Archer et al., 2020; Rousselet et al., 2019). A previous high-resolution study of the physical processes around fronts on the boundary of mesoscale eddies in this region found that frontal subduction coupled with strong temperature gradients is a persistent feature and it's likely these processes may be responsible for some of the patterns observed in the current study (Archer et al., 2020).

While this study provides the first high-resolution depth resolved cross-shelf transects in the EAC region, it is limited to the top 100 m of the water column and there may be some influence of diel vertical migration of zooplankton on the vertical distribution. Our comparison of day and night samples showed minimal differences (Figure S3 in Supporting Information S1), suggesting that the results are robust in terms of any impacts of vertical migration. As inshore water masses are more influenced by terrestrial inputs, waves, wind driven vertical mixing and we did not sample in areas with bathymetry less than 50 m, our study does not consider these inshore processes and further research is needed into the inshore processes and how these may influence particle distributions.

4.2. Comparison to Other Studies

Our study showed a consistent decline in biomass (m^{-3}) with increasing distance from shore and with increasing depth (to 100 m depth) with the largest biomasses observed in the surface inner shelf waters (bathymetry <100 m), likely due to coastal nutrient enrichment (from a variety of mechanisms). This was similar to almost all other comparable studies with the exception being the western Mediterranean (Sabatès et al., 1989). Despite different regional dynamics, cross-shelf and vertical gradients in water masses (here driven by the EAC and uplift) seem to be the dominant factor for the patterns observed at various locations worldwide. In the northeast Atlantic, the declining pattern of biomass across the shelf was attributed to coastal nutrient inputs and long residence times of water masses over the shelf break (Irigoien et al., 2009; Sourisseau & Carlotti, 2006; Vandromme et al., 2014). However, in the Brazilian Bight (southwest Atlantic), the increase in inshore zooplankton biomass was attributed to bottom intrusions of cooler nutrient rich South Atlantic central water (Pereira Brandini et al., 2014). Further south of the Brazilian Bight, similar results were observed on the Abrolhos Bank where higher zooplankton biomass was observed on the continental shelf due to the Brazil Current interacting with the sea-floor, generating uplift and eddies which increased mixing over the continental shelf (Marcolin et al., 2013). The Abrolhos Bank also showed a declining pattern in vertical zooplankton distribution similar to that observed in the particulates in the present study (Marcolin et al., 2015).

In the southwest Pacific, there are relatively small terrestrial influences compared to other sources of nutrients such as upwelling (Apte et al., 1998; Dai & Trenberth, 2002; Pritchard et al., 2003; Suthers et al., 2011). Similar to the Brazil Current and the Abrolhos bank, the EAC interacts with the topography which in turn generates uplift of cooler water onto the continental shelf (Roughan & Middleton, 2002).

A steeper size spectrum slope in inshore regions is another feature of zooplankton communities which are consistently observed. In some regions, the areas of steepest slopes have been linked to estuarine-derived nutrients (Irigoien et al., 2009; Moore & Suthers, 2006), which are exploited by nearshore planktonic communities. Within the cross-shelf patterns of zooplankton, biomass, and mean size also tend to decline with depth in the water column.

There are exceptions to the general trends that we identified in biomass, abundance, and size spectrum slope. For example, Nogueira et al. (2004) showed a shallow inshore slope compared to offshore, which was attributed to nearby continental inputs increasing the proportion of large zooplankton possibly due to a mesotrophic environment where energy transfer is highly efficient (Atkinson et al., 2021). Some studies also show these onshore-offshore gradients are highly variable as observed in the East China Sea where onshore-offshore gradients in different years showed no consistency, but insufficient data were provided for these samples to be included in our analysis (García-Comas et al., 2014). This temporal instability in some regions suggests that repeated surveys under different oceanographic conditions may be necessary to fully understand the drivers of zooplankton on continental shelfs. The long-term cross-shelf survey in the northeast Pacific may provide a good template for seasonal surveys (Kwong et al., 2022), and demonstrated stability in the cross-shelf zooplankton patterns. The current study had no temporal replication and while it was shown that the conditions which were sampled are regularly occurring features in terms of both upwelling (Schaeffer & Roughan, 2015), EAC influence and chlorophyll production (Everett et al., 2014), additional studies would be useful to confirm the regular occurrence of the patterns in particulate biomass and size structure.

While none of the previous studies have examined the vertical structure of continental shelf zooplankton communities in the same detail as horizontal structure, several studies, with coarser vertical resolution, have made similar conclusions to that observed in the current study. In the southeast Atlantic, a higher biomass of zooplankton was found above the pycnocline attributed to the increased chlorophyll a in these waters (Marcolin et al., 2013). In the northwest Atlantic, a similar strong association was found with a thermocline, with distinct zooplankton communities across the continental shelf separated by the 15°C thermocline (Turner & Dagg, 1983). Similar patterns in zooplankton size structure are observed around thermoclines in subtropical Australia (Suthers et al., 2006). The high vertical and horizontal resolution of the current study is advantageous as we can look at both vertical and horizontal patterns in great context than traditional point-based sampling, for example, we now have the potential to visualize particulate patterns vary around isotherms as they upwell onto continental shelves.

When the abundance and biomass ratios were calculated with a per m^2 metric to investigate overall plankton abundance and biomass in the water column, the inshore-offshore gradients disappeared. This suggests there may be some physical effect of the particulate community being concentrated in a shallower water column. Regardless, the size spectrum slope estimates are independent of water column depth and these in themselves suggest the zooplankton and particulate communities differ substantially inshore and offshore. It is most likely both a combination of physical concentration and different populations dynamics shaping the cross-shelf differences in particulate size structure.

4.3. Implications for the Future

While the distributions and patterns observed in the current study align with global observations, they are only a snapshot and at other times of the year the patterns may vary. The velocities observed in our study reflect a large portion of the year in terms of the velocities at our transect locations (Figure 2). Despite this, the EAC is strengthening (Suthers et al., 2011; Wu et al., 2012), and the increasing water temperatures in the southeast Australian region (Malan et al., 2021), are already impacting the zooplankton communities as the region becomes increasingly tropicalized (Kelly et al., 2016). At long-term observing stations in the southeast Australian region, warming waters have resulted in a reduction in the spring phytoplankton bloom and >60% decline phytoplankton growth during spring (Thompson et al., 2009). These changes may have significant bottom-up effects on the overall distribution of particulate biomass, size structure and community composition on continental shelves as

zooplankton are impacted across the globe in similar ways (Richardson, 2008). With the impacts of warming oceans already being observed at coastal observing stations and phytoplankton communities increasingly dominated by warm-water tolerant chain forming diatoms (Ajani et al., 2020), impacts from projected reductions in both phytoplankton and zooplankton biomass are likely to be amplified up the food web with potentially large impacts on fisheries. If we hypothesize based upon the results of the current study and the EAC warming and penetrating further south as already being observed (Li et al., 2022; Malan et al., 2021; Wu et al., 2012), it is likely that particulate communities may show reduced biomass, and larger mean sizes with more efficient trophic transfer of energy as the warm EAC water displaces the cooler more productive Tasman Sea waters.

Using an OPC allowed for the size distribution of particles across the continental shelf to be vertically resolved here. However, given OPCs are only capable of detecting the abundance and size of nondescript particles, their biological composition (i.e., what percentage are nonliving aggregates, phytoplankton or zooplankton?) is unknown. As such, this should be considered in relation to the causal drivers of trends we have discussed. While size spectra from OPCs have previously been used as a direct proxy for the size structure of plankton (Everett et al., 2017; Kwong et al., 2022; Wallis et al., 2016), some studies suggest that the proportion of particulates comprised of plankton may be in the minority. For example, comparing in situ OPC counts with samples collected with plankton nets off southern California, González-Quirós and Checkley (2006) found only a third of the particles by volume were retained in plankton nets suggesting the difference was owing to fragile biogenic nonliving aggregates not being collected. Stemmann and Boss (2012) suggest that as much as 85%–99% of particulates across the zooplankton size range are likely to be nonliving. While exact contributions of nonliving and living particulates in marine size spectra are not well known, this is challenging for our interpretation of planktonic size spectra dynamics here whereby organisms start small and grow as energy is transferred up size classes through predation (Blanchard et al., 2017; Heneghan et al., 2019), given nonliving aggregates can originate as either small or large and decrease or increase in size through coagulation or disintegration processes, respectively (Stemmann & Boss, 2012). Despite this, our results indicate that trends in size spectra described here are likely driven at least in-part by dynamics of living particles owing to the relationship between nutrient enrichment, chlorophyll a concentration, and steeper size spectra we have discussed (e.g., Figure 6 and Figures S9, S10 in Supporting Information S1). Since the transects used in this study were conducted, there have been large technological advancements in towed plankton sampling gear, such as the in situ Ichthyoplankton Imaging System (ISIIS; Cowen & Guigand, 2008) or the Continuous Plankton Imaging and Classification Sensor (CPICS; Grossmann et al., 2015), which allow the taxonomic composition of particles to be identified using machine learning and image analysis (Lombard et al., 2019). Consequently, it is possible for future studies to expand on the global patterns in cross-shelf particle distribution we have described (e.g., Figure 7) to better understand how these patterns relate to productivity of plankton in the coastal ocean.

5. Conclusions

Based upon the general cross-shelf patterns and the depth resolved data from the present study, we suggest a general process for the distribution of planktonic particles on continental shelves influenced by boundary currents (Figure 8), although we also showed fronts between water masses can disrupt general inshore-offshore trends. This heuristic model includes expectations for future studies to examine, such as the decline in biomass with distance offshore and with depth in the water column. This is potentially driven by cross-shelf differences in nutrient input which in our area was driven by the East Australia Current, which drives productivity on the shelf through uplift of nutrient rich waters. Future studies could answer these questions with more sustained monitoring of cross-shelf patterns in size structure throughout the year.

Conflict of Interest

The authors declare no conflicts of interest relevant to this study.

Data Availability Statement

All data used in this study are freely accessible. The data from the Southern Surveyor voyage 08/2004 are available from the CSIRO Data Trawler (https://www.marine.csiro.au/data/trawler/). The long-term environmental data is available from the Australian Ocean Data Network (https://portal.aodn.org.au/). All code used for the analysis in this paper is available in the Zenodo repository (H. T. Schilling, 2022).

Acknowledgments
The authors wish to thank the Marine National Facility, the captain and crew of *RV Southern Surveyor* 08/2004, chief scientist Jason Middleton and especially voyage manager Lindsey Pender. HTS was supported by a NSW Government Research Attraction and Acceleration Program grant awarded to SIMS. This paper is SIMS publication #302. This research was funded by ARC Discovery Projects DP0209193 held by IMS and MEB, DP0208663 held by Jason Middleton, and DP0557618 held by MEB. JDE was supported by DP150102656 and DP190102293. Satellite data were sourced from Australia's Integrated Marine Observing System (IMOS)—IMOS is enabled by the National Collaborative Research Infrastructure strategy (NCRIS). Open access publishing facilitated by University of New South Wales, as part of the Wiley - University of New South Wales agreement via the Council of Australian University Librarians.

References

Aguiar, A. L., Cirano, M., Pereira, J., & Marta-Almeida, M. (2014). Upwelling processes along a Western boundary current in the Abrolhos-Campos region of Brazil. *Continental Shelf Research*, *85*, 42–59. https://doi.org/10.1016/j.csr.2014.04.013

Ajani, P. A., Davies, C. H., Eriksen, R. S., & Richardson, A. J. (2020). Global warming impacts micro-phytoplankton at a long-term Pacific ocean coastal station. *Frontiers in Marine Science*, *7*, 576011. https://doi.org/10.3389/fmars.2020.576011

Akima, H., & Gebhardt, A. (2020). akima: Interpolation of irregularly and regularly spaced data. R package version 0.6-2.1. (Version R package version 0.6-2.1). Retrieved from https://CRAN.R-project.org/package=akima

Andersen, K. H., Berge, T., Gonçalves, R. J., Hartvig, M., Heuschele, J., Hylander, S., et al. (2016). Characteristic sizes of life in the oceans, from bacteria to whales. *Annual Review of Marine Science*, *8*(1), 217–241. https://doi.org/10.1146/annurev-marine-122414-034144

Apte, S. C., Batley, G. E., Szymczak, R., Rendell, P. S., Lee, R., & Waite, T. D. (1998). Baseline trace metal concentrations in New South Wales coastal waters. *Marine and Freshwater Research*, *49*(3), 203–214. https://doi.org/10.1071/mf96121

Archer, M. R., Roughan, M., Keating, S. R., & Schaeffer, A. (2017). On the variability of the East Australian current: Jet structure, meandering, and influence on shelf circulation. *Journal of Geophysical Research: Oceans*, *122*, 8464–8481. https://doi.org/10.1002/2017JC013097

Archer, M. R., Schaeffer, A., Keating, S., Roughan, M., Holmes, R., & Siegelman, L. (2020). Observations of submesoscale variability and frontal subduction within the mesoscale eddy field of the Tasman Sea. *Journal of Physical Oceanography*, *50*(5), 1509–1529. https://doi.org/10.1175/JPO-D-19-0131.1

Armbrecht, L. H., Roughan, M., Rossi, V., Schaeffer, A., Davies, P. L., Waite, A. M., & Armand, L. K. (2014). Phytoplankton composition under contrasting oceanographic conditions: Upwelling and downwelling (Eastern Australia). *Continental Shelf Research*, *75*, 54–67. https://doi.org/10.1016/j.csr.2013.11.024

Armbrecht, L. H., Thompson, P. A., Wright, S. W., Schaeffer, A., Roughan, M., Henderiks, J., & Armand, L. K. (2015). Comparison of the cross-shelf phytoplankton distribution of two oceanographically distinct regions off Australia. *Journal of Marine Systems*, *148*, 26–38. https://doi.org/10.1016/j.jmarsys.2015.02.002

Atkinson, A., Lilley, M. K. S., Hirst, A. G., McEvoy, A. J., Tarran, G. A., Widdicombe, C., et al. (2021). Increasing nutrient stress reduces the efficiency of energy transfer through planktonic size spectra. *Limnology & Oceanography*, *66*(2), 422–437. https://doi.org/10.1002/lno.11613

Baird, M. E., Timko, P. G., Middleton, J. H., Mullaney, T. J., Cox, D. R., & Suthers, I. M. (2008). Biological properties across the Tasman front off southeast Australia. *Deep Sea Research Part I: Oceanographic Research Papers*, *55*(11), 1438–1455. https://doi.org/10.1016/j.dsr.2008.06.011

Bakun, A., & Weeks, S. J. (2008). The marine ecosystem off Peru: What are the secrets of its fishery productivity and what might its future hold? *Progress in Oceanography*, *79*(2–4), 290–299. https://doi.org/10.1016/j.pocean.2008.10.027

Barnes, C., Maxwell, D., Reuman, D. C., & Jennings, S. (2010). Global patterns in predator-prey size relationships reveal size dependency of trophic transfer efficiency. *Ecology*, *91*(1), 222–232. https://doi.org/10.1890/08-2061.1

Blanchard, J. L., Heneghan, R. F., Everett, J. D., Trebilco, R., & Richardson, A. J. (2017). From bacteria to whales: Using functional size spectra to model marine ecosystems. *Trends in Ecology & Evolution*, *32*(3), 174–186. https://doi.org/10.1016/j.tree.2016.12.003

Carr, M.-E., & Kearns, E. J. (2003). Production regimes in four eastern boundary current systems. *Deep Sea Research Part II: Topical Studies in Oceanography*, *50*(22), 3199–3221. https://doi.org/10.1016/j.dsr2.2003.07.015

Cetina-Heredia, P., Roughan, M., van Sebille, E., & Coleman, M. A. (2014). Long-term trends in the East Australian Current separation latitude and eddy driven transport. *Journal of Geophysical Research: Oceans*, *119*, 4351–4366. https://doi.org/10.1002/2014JC010071

Correll, D. L., Jordan, T. E., & Weller, D. E. (1992). Nutrient flux in a landscape: Effects of coastal land use and terrestrial community mosaic on nutrient transport to coastal waters. *Estuaries*, *15*(4), 431–442. https://doi.org/10.2307/1352388

Cowen, R. K., & Guigand, C. M. (2008). In situ ichthyoplankton imaging system (ISIIS): System design and preliminary results. *Limnology and Oceanography: Methods*, *6*(2), 126–132. https://doi.org/10.4319/lom.2008.6.126

Cowley, R. (1999). *Hydrochemistry operations manual (CSIRO Marine Laboratories No. 236*, (p. 106). CSIRO Division of Marine Research. https://doi.org/10.4225/08/585d676eb38c9

Dai, A., & Trenberth, K. E. (2002). Estimates of freshwater discharge from continents: Latitudinal and seasonal variations. *Journal of Hydrometeorology*, *3*(6), 660–687. https://doi.org/10.1175/1525-7541(2002)003<0660:EOFDFC>2.0.CO;2

Edwards, A. M., Robinson, J. P. W., Plank, M. J., Baum, J. K., & Blanchard, J. L. (2017). Testing and recommending methods for fitting size spectra to data. *Methods in Ecology and Evolution*, *8*(1), 57–67. https://doi.org/10.1111/2041-210X.12641

Everett, J. D., Baird, M. E., Buchanan, P., Bulman, C., Davies, C., Downie, R., et al. (2017). Modeling what we sample and sampling what we model: Challenges for zooplankton model assessment. *Frontiers in Marine Science*, *4*, 77. https://doi.org/10.3389/fmars.2017.00077

Everett, J. D., Baird, M. E., Oke, P. R., & Suthers, I. M. (2012). An avenue of eddies: Quantifying the biophysical properties of mesoscale eddies in the Tasman Sea. *Geophysical Research Letters*, *39*, L16608. https://doi.org/10.1029/2012GL053091

Everett, J. D., Baird, M. E., Roughan, M., Suthers, I. M., & Doblin, M. A. (2014). Relative impact of seasonal and oceanographic drivers on surface chlorophyll *a* along a Western Boundary Current. *Progress in Oceanography*, *120*, 340–351. https://doi.org/10.1016/j.pocean.2013.10.016

García-Comas, C., Chang, C.-Y., Ye, L., Sastri, A. R., Lee, Y.-C., Gong, G.-C., & Hsieh, C. (2014). Mesozooplankton size structure in response to environmental conditions in the East China Sea: How much does size spectra theory fit empirical data of a dynamic coastal area? *Progress in Oceanography*, *121*, 141–157. https://doi.org/10.1016/j.pocean.2013.10.010

GEBCO Bathymetric Compilation Group. (2019). *The GEBCO_2019 Grid—A continuous terrain model of the global oceans and land*. British Oceanographic Data Centre, National Oceanography Centre.

González-Quirós, R., & Checkley, D. M. (2006). Occurrence of fragile particles inferred from optical plankton counters used in situ and to analyze net samples collected simultaneously. *Journal of Geophysical Research*, *111*, C05S06. https://doi.org/10.1029/2005JC003084

Grossmann, M. M., Gallager, S. M., & Mitarai, S. (2015). Continuous monitoring of near-bottom mesoplankton communities in the East China Sea during a series of typhoons. *Journal of Oceanography*, *71*(1), 115–124. https://doi.org/10.1007/s10872-014-0268-y

Guiet, J., Poggiale, J.-C., & Maury, O. (2016). Modelling the community size-spectrum: Recent developments and new directions. *Ecological Modelling*, *337*, 4–14. https://doi.org/10.1016/j.ecolmodel.2016.05.015

Hamner, W. M., Jones, M. S., Carleton, J. H., Hauri, I. R., & Williams, D. M. (1988). Zooplankton, planktivorous fish, and water currents on a windward reef face—Great Barrier Reef, Australia. *Bulletin of Marine Science*, *42*(3), 459–479.

Heneghan, R. F., Hatton, I. A., & Galbraith, E. D. (2019). Climate change impacts on marine ecosystems through the lens of the size spectrum. *Emerging Topics in Life Sciences*, *3*(2), 233–243. https://doi.org/10.1042/ETLS20190042

Herman, A. W. (1992). Design and calibration of a new optical plankton counter capable of sizing small zooplankton. *Deep Sea Research, Part A: Oceanographic Research Papers*, *39*(3), 395–415. https://doi.org/10.1016/0198-0149(92)90080-D

Hobday, A. J., & Hartmann, K. (2006). Near real-time spatial management based on habitat predictions for a longline bycatch species. *Fisheries Management and Ecology*, *13*(6), 365–380. https://doi.org/10.1111/j.1365-2400.2006.00515.x

Holland, M. M., Everett, J. D., Cox, M. J., Doblin, M. A., & Suthers, I. M. (2021). Pelagic forage fish distribution in a dynamic shelf ecosystem—Thermal demands and zooplankton prey distribution. *Estuarine, Coastal and Shelf Science*, *249*, 107074. https://doi.org/10.1016/j.ecss.2020.107074

Holland, M. M., Smith, J. A., Everett, J. D., Vergés, A., & Suthers, I. M. (2020). Latitudinal patterns in trophic structure of temperate reef-associated fishes and predicted consequences of climate change. *Fish and Fisheries*, *21*, 1092–1108. https://doi.org/10.1111/faf.12488

Irigoien, X., Fernandes, J. A., Grosjean, P., Denis, K., Albaina, A., & Santos, M. (2009). Spring zooplankton distribution in the Bay of Biscay from 1998 to 2006 in relation with anchovy recruitment. *Journal of Plankton Research*, *31*(1), 1–17. https://doi.org/10.1093/plankt/fbn096

Jeffrey, S. W., & Humphrey, G. F. (1975). New spectrophotometric equations for determining chlorophylls a, b, c1 and c2 in higher plants, algae and natural phytoplankton. *Biochemie und Physiologie der Pflanzen*, *167*(2), 191–194. https://doi.org/10.1016/S0015-3796(17)30778-3

Kelly, P., Clementson, L., Davies, C., Corney, S., & Swadling, K. (2016). Zooplankton responses to increasing sea surface temperatures in the southeastern Australia global marine hotspot. *Estuarine, Coastal and Shelf Science*, *180*, 242–257. https://doi.org/10.1016/j.ecss.2016.07.019

Kobari, T., Makihara, W., Kawafuchi, T., Sato, K., & Kume, G. (2018). Geographic variability in taxonomic composition, standing stock, and productivity of the mesozooplankton community around the Kuroshio Current in the East China Sea. *Fisheries Oceanography*, *27*(4), 336–350. https://doi.org/10.1111/fog.12256

Krupica, K. L., Sprules, W. G., & Herman, A. W. (2012). The utility of body size indices derived from optical plankton counter data for the characterization of marine zooplankton assemblages. *Continental Shelf Research*, *36*, 29–40. https://doi.org/10.1016/j.csr.2012.01.008

Kwong, L. E., Ross, T., Lüskow, F., Florko, K. R. N., & Pakhomov, E. A. (2022). Spatial, seasonal, and climatic variability in mesozooplankton size spectra along a coastal-to-open ocean transect in the subarctic Northeast Pacific. *Progress in Oceanography*, *201*, 102728. https://doi.org/10.1016/j.pocean.2021.102728

Lampert, W. (1989). The adaptive significance of diel vertical migration of zooplankton. *Functional Ecology*, *3*(1), 21–27. https://doi.org/10.2307/2389671

Li, J., Roughan, M., & Kerry, C. (2022). Drivers of ocean warming in the Western boundary currents of the Southern Hemisphere. *Nature Climate Change*, *12*, 901–909. https://doi.org/10.1038/s41558-022-01473-8

Lombard, F., Boss, E., Waite, A. M., Vogt, M., Uitz, J., Stemmann, L., et al. (2019). Globally consistent quantitative observations of planktonic ecosystems. *Frontiers in Marine Science*, *6*, 196. https://doi.org/10.3389/fmars.2019.00196

Lucas, A. J., Dupont, C. L., Tai, V., Largier, J. L., Palenik, B., & Franks, P. J. S. (2011). The green ribbon: Multiscale physical control of phytoplankton productivity and community structure over a narrow continental shelf. *Limnology & Oceanography*, *56*(2), 611–626. https://doi.org/10.4319/lo.2011.56.2.0611

Mackinson, S., Daskalov, G., Heymans, J. J., Neira, S., Arancibia, H., Zetina-Rejón, M., et al. (2009). Which forcing factors fit? Using ecosystem models to investigate the relative influence of fishing and changes in primary productivity on the dynamics of marine ecosystems. *Ecological Modelling*, *220*(21), 2972–2987. https://doi.org/10.1016/j.ecolmodel.2008.10.021

Maia, H. A., Morais, R. A., Quimbayo, J. P., Dias, M. S., Sampaio, C. L. S., Horta, P. A., et al. (2018). Spatial patterns and drivers of fish and benthic reef communities at São Tomé Island, Tropical Eastern Atlantic. *Marine Ecology*, *39*(6), e12520. https://doi.org/10.1111/maec.12520

Malan, N., Archer, M., Roughan, M., Cetina-Heredia, P., Hemming, M., Rocha, C., et al. (2020). Eddy-driven cross-shelf transport in the East Australian Current separation zone. *Journal of Geophysical Research: Oceans*, *125*, e2019JC015613. https://doi.org/10.1029/2019JC015613

Malan, N., Roughan, M., & Kerry, C. (2021). The rate of coastal temperature rise adjacent to a warming Western boundary current is nonuniform with latitude. *Geophysical Research Letters*, *48*, e2020GL090751. https://doi.org/10.1029/2020GL090751

Marcolin, C. R., Lopes, R. M., & Jackson, G. A. (2015). Estimating zooplankton vertical distribution from combined LOPC and ZooScan observations on the Brazilian Coast. *Marine Biology*, *162*(11), 2171–2186. https://doi.org/10.1007/s00227-015-2753-2

Marcolin, C. R., Schultes, S., Jackson, G. A., & Lopes, R. M. (2013). Plankton and seston size spectra estimated by the LOPC and ZooScan in the Abrolhos Bank ecosystem (SE Atlantic). *Continental Shelf Research*, *70*, 74–87. https://doi.org/10.1016/j.csr.2013.09.022

Marshak, A. R., & Link, J. S. (2021). Primary production ultimately limits fisheries economic performance. *Scientific Reports*, *11*(1), 12154. https://doi.org/10.1038/s41598-021-91599-0

Mitra, A., Castellani, C., Gentleman, W. C., Jónasdóttir, S. H., Flynn, K. J., Bode, A., et al. (2014). Bridging the gap between marine biogeochemical and fisheries sciences; configuring the zooplankton link. *Progress in Oceanography*, *129*, 176–199. https://doi.org/10.1016/j.pocean.2014.04.025

Moore, S. K., & Suthers, I. M. (2006). Evaluation and correction of subresolved particles by the optical plankton counter in three Australian estuaries with pristine to highly modified catchments. *Journal of Geophysical Research*, *111*, C05S04. https://doi.org/10.1029/2005JC002920

Morris, A. W., Allen, J. I., Howland, R. J. M., & Wood, R. G. (1995). The estuary plume zone: Source or sink for land-derived nutrient discharges? *Estuarine, Coastal and Shelf Science*, *40*(4), 387–402. https://doi.org/10.1006/ecss.1995.0027

Nogueira, E., González-Nuevo, G., Bode, A., Varela, M., Morán, X. A. G., & Valdés, L. (2004). Comparison of biomass and size spectra derived from optical plankton counter data and net samples: Application to the assessment of mesoplankton distribution along the Northwest and North Iberian shelf. *ICES Journal of Marine Science*, *61*(4), 508–517. https://doi.org/10.1016/j.icesjms.2004.03.018

Noyon, M., Poulton, A. J., Asdar, S., Weitz, R., & Giering, S. L. C. (2022). Mesozooplankton community distribution on the Agulhas Bank in autumn: Size structure and production. *Deep Sea Research Part II: Topical Studies in Oceanography*, *195*, 105015. https://doi.org/10.1016/j.dsr2.2021.105015

Oke, P. R., Roughan, M., Cetina-Heredia, P., Pilo, G. S., Ridgway, K. R., Rykova, T., et al. (2019). Revisiting the circulation of the East Australian Current: Its path, separation, and eddy field. *Progress in Oceanography*, *176*, 102139. https://doi.org/10.1016/j.pocean.2019.102139

Pauly, D., Christensen, V., Guénette, S., Pitcher, T. J., Sumaila, U. R., Walters, C. J., et al. (2002). Towards sustainability in world fisheries. *Nature*, *418*(6898), 689–695. https://doi.org/10.1038/nature01017

Pereira Brandini, F., Nogueira, M., Simião, M., Carlos Ugaz Codina, J., & Almeida Noernberg, M. (2014). Deep chlorophyll maximum and plankton community response to oceanic bottom intrusions on the continental shelf in the South Brazilian Bight. *Continental Shelf Research*, *89*, 61–75. https://doi.org/10.1016/j.csr.2013.08.002

Pritchard, T. R., Lee, R. S., Ajani, P. A., Rendell, P. S., Black, K., & Koop, K. (2003). Phytoplankton responses to nutrient sources in coastal waters off southeastern Australia. *Aquatic Ecosystem Health and Management*, *6*(2), 105–117. https://doi.org/10.1080/14634980301469

R Core Team. (2020). R: A language and environment for statistical computing v4.0.2. *R Foundation for Statistical Computing*.

Revill, A. T., Young, J. W., & Lansdell, M. (2009). Stable isotopic evidence for trophic groupings and bio-regionalization of predators and their prey in oceanic waters off eastern Australia. *Marine Biology*, *156*(6), 1241–1253. https://doi.org/10.1007/s00227-009-1166-5

Richardson, A. J. (2008). In hot water: Zooplankton and climate change. *ICES Journal of Marine Science*, *65*(3), 279–295. https://doi.org/10.1093/icesjms/fsn028

Ridgway, K. R., & Dunn, J. R. (2003). Mesoscale structure of the mean East Australian Current System and its relationship with topography. *Progress in Oceanography*, *56*(2), 189–222. https://doi.org/10.1016/S0079-6611(03)00004-1

Rocha, C., Edwards, C. A., Roughan, M., Cetina-Heredia, P., & Kerry, C. (2019). A high-resolution biogeochemical model (ROMS 3.4 + bio_Fennel) of the East Australian Current system. *Geoscientific Model Development*, *12*(1), 441–456. https://doi.org/10.5194/gmd-12-441-2019

Rossberg, A. G., Gaedke, U., & Kratina, P. (2019). Dome patterns in pelagic size spectra reveal strong trophic cascades. *Nature Communications*, *10*(1), 4396. https://doi.org/10.1038/s41467-019-12289-0

Rossi, V., Schaeffer, A., Wood, J., Galibert, G., Morris, B., Sudre, J., et al. (2014). Seasonality of sporadic physical processes driving temperature and nutrient high-frequency variability in the coastal ocean off southeast Australia. *Journal of Geophysical Research: Oceans*, *119*, 445–460. https://doi.org/10.1002/2013JC009284

Roughan, M., & Middleton, J. H. (2002). A comparison of observed upwelling mechanisms off the East Coast of Australia. *Continental Shelf Research*, *22*(17), 2551–2572. https://doi.org/10.1016/s0278-4343(02)00101-2

Rousselet, L., Doglioli, A. M., de Verneil, A., Pietri, A., Della Penna, A., Berline, L., et al. (2019). Vertical motions and their effects on a biogeochemical tracer in a cyclonic structure finely observed in the Ligurian sea. *Journal of Geophysical Research: Oceans*, *124*, 3561–3574. https://doi.org/10.1029/2018JC014392

Sabatès, A., Gili, J. M., & Pagès, F. (1989). Relationship between zooplankton distribution, geographic characteristics and hydrographic patterns off the Catalan coast (Western Mediterranean). *Marine Biology*, *103*(2), 153–159. https://doi.org/10.1007/BF00543342

Schaeffer, A., Gramoulle, A., Roughan, M., & Mantovanelli, A. (2017). Characterizing frontal eddies along the East Australian Current from HF radar observations. *Journal of Geophysical Research: Oceans*, *122*, 3964–3980. https://doi.org/10.1002/2016JC012171

Schaeffer, A., & Roughan, M. (2015). Influence of a Western boundary current on shelf dynamics and upwelling from repeat glider deployments. *Geophysical Research Letters*, *42*, 121–128. https://doi.org/10.1002/2014GL062260

Schaeffer, A., Roughan, M., & Morris, B. D. (2013). Cross-shelf dynamics in a Western boundary current regime: Implications for upwelling. *Journal of Physical Oceanography*, *44*(10), 2812–2813. https://doi.org/10.1175/JPO-D-14-0091.1

Schaeffer, A., Roughan, M., & Wood, J. E. (2014). Observed bottom boundary layer transport and uplift on the continental shelf adjacent to a Western boundary current. *Journal of Geophysical Research: Oceans*, *119*, 4922–4939. https://doi.org/10.1002/2013JC009735

Schilling, H., Smith, J., Everett, J., Harrison, D., Suthers, I., Schilling, H., et al. (2022). Size selective predation by three estuarine zooplanktivorous fish species. *Marine and Freshwater Research*, *73*(6), 823–832. https://doi.org/10.1071/MF21344

Schilling, H. T. (2022). *Data and Code accompanying Schilling et al., Vertically resolved planktonic particle biomass and size-structure across a continental shelf under the influence of a western boundary current*. Zenodo. https://doi.org/10.5281/zenodo.7259671

Sourisseau, M., & Carlotti, F. (2006). Spatial distribution of zooplankton size spectra on the French continental shelf of the Bay of Biscay during spring 2000 and 2001. *Journal of Geophysical Research*, *111*, C05S09. https://doi.org/10.1029/2005JC003063

Sprules, W. G., & Barth, L. E. (2015). Surfing the biomass size spectrum: Some remarks on history, theory, and application. *Canadian Journal of Fisheries and Aquatic Sciences*, *73*(4), 477–495. https://doi.org/10.1139/cjfas-2015-0115

Stemmann, L., & Boss, E. (2012). Plankton and particle size and packaging: From determining optical properties to driving the biological pump. *Annual Review of Marine Science*, *4*(1), 263–290. https://doi.org/10.1146/annurev-marine-120710-100853

Suthers, I. M., Taggart, C. T., Rissik, D., & Baird, M. E. (2006). Day and night ichthyoplankton assemblages and zooplankton biomass size spectrum in a deep ocean island wake. *Marine Ecology Progress Series*, *322*, 225–238. https://doi.org/10.3354/meps322225

Suthers, I. M., Young, J. W., Baird, M. E., Roughan, M., Everett, J. D., Brassington, G. B., et al. (2011). The strengthening East Australian Current, its eddies and biological effects—An introduction and overview. *Deep Sea Research Part II: Topical Studies in Oceanography*, *58*(5), 538–546. https://doi.org/10.1016/j.dsr2.2010.09.029

Thompson, P. A., Baird, M. E., Ingleton, T., & Doblin, M. A. (2009). Long-term changes in temperate Australian coastal waters: Implications for phytoplankton. *Marine Ecology Progress Series*, *394*, 1–19. https://doi.org/10.3354/meps08297

Truong, L., Suthers, I. M., Cruz, D. O., & Smith, J. A. (2017). Plankton supports the majority of fish biomass on temperate rocky reefs. *Marine Biology*, *164*(4), 12. https://doi.org/10.1007/s00227-017-3101-5

Turner, J. T., & Dagg, M. J. (1983). Vertical distributions of continental shelf zooplankton in stratified and isothermal waters. *Biological Oceanography*, *3*(1), 1–40. https://doi.org/10.1080/01965581.1983.10749470

Vandromme, P., Nogueira, E., Huret, M., Lopez-Urrutia, Á., González, G. G.-N., Sourisseau, M., & Petitgas, P. (2014). Springtime zooplankton size structure over the continental shelf of the Bay of Biscay. *Ocean Science*, *10*(5), 821–835. https://doi.org/10.5194/os-10-821-2014

Vidondo, B., Prairie, Y. T., Blanco, J. M., & Duarte, C. M. (1997). Some aspects of the analysis of size spectra in aquatic ecology. *Limnology & Oceanography*, *42*(1), 184–192. https://doi.org/10.4319/lo.1997.42.1.0184

Wallis, J. R., Swadling, K. M., Everett, J. D., Suthers, I. M., Jones, H. J., Buchanan, P. J., et al. (2016). Zooplankton abundance and biomass size spectra in the East Antarctic sea-ice zone during the winter-spring transition. *Deep Sea Research Part II: Topical Studies in Oceanography*, *131*, 170–181. https://doi.org/10.1016/j.dsr2.2015.10.002

White, E. P., Ernest, S. K. M., Kerkhoff, A. J., & Enquist, B. J. (2007). Relationships between body size and abundance in ecology. *Trends in Ecology & Evolution*, *22*(6), 323–330. https://doi.org/10.1016/j.tree.2007.03.007

Wickham, H. (2011). ggplot2. *WIREs Computational Statistics*, *3*(2), 180–185. https://doi.org/10.1002/wics.147

Wood, J. E., Roughan, M., & Tate, P. M. (2012). Finding a proxy for wind stress over the coastal ocean. *Marine and Freshwater Research*, *63*(6), 528–544. https://doi.org/10.1071/MF11250

Wu, L., Cai, W., Zhang, L., Nakamura, H., Timmermann, A., Joyce, T., et al. (2012). Enhanced warming over the global subtropical Western boundary currents. *Nature Climate Change*, *2*(3), 161–166. https://doi.org/10.1038/nclimate1353

Zhou, M. (2006). What determines the slope of a plankton biomass spectrum? *Journal of Plankton Research*, *28*(5), 437–448. https://doi.org/10.1093/plankt/fbi119

References From the Supporting Information

Becker, É. C., Eiras Garcia, C. A., & Freire, A. S. (2018). Mesozooplankton distribution, especially copepods, according to water masses dynamics in the upper layer of the Southwestern Atlantic shelf (26°S to 29°S). *Continental Shelf Research*, *166*, 10–21. https://doi.org/10.1016/j.csr.2018.06.011

Beckley, L. E., Holliday, D., Sutton, A. L., Weller, E., Olivar, M. P., & Thompson, P. A. (2018). Structuring of larval fish assemblages along a coastal-oceanic gradient in the macro-tidal, tropical Eastern Indian Ocean. *Deep Sea Research Part II: Topical Studies in Oceanography*, *161*, 105–119. https://doi.org/10.1016/j.dsr2.2018.03.008

Coyle, K. O., & Pinchuk, A. I. (2005). Seasonal cross-shelf distribution of major zooplankton taxa on the northern Gulf of Alaska shelf relative to water mass properties, species depth preferences and vertical migration behavior. *Deep Sea Research Part II: Topical Studies in Oceanography*, *52*(1–2), 217–245. https://doi.org/10.1016/j.dsr2.2004.09.025

García-Muñoz, C., García, C. M., Lubián, L. M., López-Urrutia, Á., Hernández-León, S., & Ameneiro, J. (2014). Metabolic state along a summer northnorth-south transect near the Antarctic Peninsula: A size spectra approach. *Journal of Plankton Research*, *36*(4), 1074–1091. https://doi.org/10.1093/plankt/fbu042

Lopes, R. M., Katsuragawa, M., Dias, J. F., Montú, M. A., Muelbert, J. H., Gorri, C., & Brandini, F. P. (2006). Zooplankton and ichthyoplankton distribution on the southern Brazilian shelf: An overview. *Scientia Marina*, *70*(2), 14–202. https://doi.org/10.3989/scimar.2006.70n2189

Schultes, S., & Lopes, R. M. (2009). Laser Optical Plankton Counter and Zooscan intercomparison in tropical and subtropical marine ecosystems. *Limnology and Oceanography: Methods*, *7*(11), 771–784. https://doi.org/10.4319/lom.2009.7.771

Skarðhamar, J., Slagstad, D., & Edvardsen, A. (2007). Plankton distributions related to hydrography and circulation dynamics on a narrow continental shelf off Northern Norway. *Estuarine, Coastal and Shelf Science*, *75*(3), 381–392. https://doi.org/10.1016/j.ecss.2007.05.044

Zeldis, J. R., & Willis, K. J. (2015). Biogeographic and trophic drivers of mesozooplankton distribution on the northeast continental shelf and in Hauraki Gulf, New Zealand. *New Zealand Journal of Marine & Freshwater Research*, *49*(1), 69–86. https://doi.org/10.1080/00288330.2014.955806

Zhang, W., Sun, X., Zheng, S., Zhu, M., Liang, J., Du, J., & Yang, C. (2019). Plankton abundance, biovolume, and normalized biovolume size spectra in the northern slope of the South China Sea in autumn 2014 and summer 2015. *Deep Sea Research Part II: Topical Studies in Oceanography*, *167*, 79–92. https://doi.org/10.1016/j.dsr2.2019.07.006